THERMAL PERFORMANCE AND SIMULATION ANALYSIS OF SOLAR UPDRAFT TOWER

A DISSERTATION

SUBMITTED IN PARTIAL FULFILLMENT OF THE REQUIREMENTS FOR THE AWARD OF THE DEGREE
OF

MASTER OF TECHNOLOGY

IN

THERMAL ENGINEERING

Submitted by:

RAHUL RATAN

(2K17/THE/11)

Under the supervision of

PROF. SAMSHER

&

DR. ANIL KUMAR

MECHANICAL ENGINEERING DEPARTMENT

DELHI TECHNOLOGICAL UNIVERSITY

(Formerly Delhi College of Engineering)

Bawana Road, Delhi-110042

October, 2019

DELHI TECHNOLOGICAL UNIVERSITY

(Formerly Delhi College of Engineering)

Bawana Road, Delhi-110042

CANDIDATE'S DECLARATION

I, Rahul Ratan, 2K17/THE/11 student of M.Tech. (Thermal Engineering), hereby declare that the project Dissertation title "Thermal Performance and Simulation Analysis of Solar Updraft Tower" which is submitted by me to the Department of Mechanical Engineering, Delhi Technological University, Delhi in partial fulfillment of the requirement for the award of the degree of Master of Technology, is original and not copied from any source without proper citation. This work has not previously formed the basis for the award of any Degree, Diploma, Associateship, Fellowship or other similar title or recognition.

Place: Delhi **RAHUL RATAN**

Date:

MECHANICAL ENGINEERING DEPARTMENT

DELHI TECHNOLOGICAL UNIVERSITY

(Formerly Delhi College of Engineering)

Bawana Road, Delhi-110042

CERTIFICATE

I hereby certify that the Project Dissertation titled "Thermal Performance and Simulation Analysis of Solar Updraft Tower" which is submitted by Rahul Ratan, 2K17/THE/11, Mechanical Engineering Department, Delhi Technological University, Delhi in partial fulfillment of the requirement for the award of the degree of Master of Technology, is a record of the project work carried out by the students under my supervision. To the best of my knowledge this work has not been submitted in part or full for any Degree or Diploma to this University or elsewhere.

Place: Delhi

Date:

PROF. SAMSHER

SUPERVISOR

Professor, Mechanical Engineering Department

Delhi Technological University, Delhi – 110042

DR. ANIL KUMAR

SUPERVISOR

Associate Professor, Mechanical Engineering Department

Delhi Technological University, Delhi – 110042

ACKNOWLEDGEMENT

I would like to thank Delhi Technological University for giving me an opportunity to learn and keep in touch with recent advances in the area of Solar Energy by supporting the research and providing an atmosphere to discuss various technology related issues.

I would like to express my heartfelt regard and gratitude to my supervisors Prof. Samsher & Dr. Anil Kumar from whom I have learnt the subject matter and which gave me inspiration to write this dissertation.

I would also like to thank Ravi Kant Sir & my friend Sudhanshu Dutta for their continuous support and motivation to pursue the research work presented in this dissertation.

RAHUL RATAN

ABSTRACT

The world community is deeply worried about the rapid depletion of fossil fuels which are not only non-renewable but also emit greenhouse gases by the combustion of fossil fuels. There can be two ways to combat such situations, the first one is the replacement of fossil fuels with renewable sources of energy and the other one is to aware the community to use the resources wisely keeping in mind the sustainable use of resources for future generations. It is very aptly said by Mahatma Gandhi "The world has enough for everyone's need, but not for anyone's greed". Using energy efficiently can reduce the use of fossil fuels but using renewable sources of energy can completely eliminate its use. Solar energy, wind energy, hydro energy, geothermal energy, and biomass energy are considered as the major sources of renewable energy. Ocean energy, tidal energy, and wave energy are also considered as sources of renewable form of energy but much work has to be done to make these energies more affordable for the common people. Among all the forms of renewable energy, Solar energy is the one which is the most popularly known renewable form of energy and mostly all other forms of renewable energy have their origin directly or indirectly from solar energy (i.e. Sun). Therefore, the sun is the ultimate source of energy and is considered as a parent which gives birth to all other forms of energy and can power the future technologies. Solar Updraft Tower is one such technology which can power the needs of the future at minimum of the cost. A decent attempt to evaluate the performance of Solar Updraft Tower has been made by setting up an experimental model on rooftop of Mechanical Engineering Department, Delhi Technological University. The maximum collector efficiency was observes as 53.48% on Day-3 at 12:00 hrs while the minimum as 10.74% on Day-1 at 8:00 hrs. The maximum chimney efficiency of 0.67% was observed on Day-2 at 17:00 hrs while the minimum chimney efficiency was observed as 0.06% on Day-1 at 11:00 hrs. The maximum overall thermal efficiency of 9.98% was observed on Day-1 at 18:00 hrs while the minimum overall thermal efficiency was observed as 1.68% on Day-1 at 09:00 hrs.

CONTENTS

LIST OF FIGURES

LIST OF TABLES

LIST OF SYMBOLS, ABBREVIATIONS & NOMENCLATURE

Nomenclature

$\dot{m}$	=	Mass Flow Rate (kg s^{-1})
c_p	=	Specific Heat Capacity (J kg^{-1} K^{-1})
T	=	Temperature (K)
I_g	=	Global Radiation (W/m^2)
A	=	Area (m^2)
g	=	Acceleration due to gravity (m s^{-2})
P	=	Power (Watts)
V	=	Voltage (Volts)
I	=	Current (Amperes)
v	=	Velocity (m s^{-1})
Ra	=	Rayleigh Number
L	=	Characteristic Length (m)
Isc	=	Solar Constant Value

Abbreviations

GMT	=	Greenwich Meridian Time
MFR	=	Mass Flow Rate
RH	=	Relative Humidity
FPC	=	Flat Plate Collectors
CPC	=	Compound Parabolic Collector
ETC	=	Evacuated Tube Collector
PTC	=	Parabolic Trough Collector
LFR	=	Linear Fresnel Reflector
PDR	=	Parabolic Dish Reflector
HFC	=	Heliostat Field Collector
SCPP	=	Solar Chimney Power Plant

SUT	=	Solar Updraft Tower
SUTPP	=	Solar Updraft Tower Power Plant
PVC	=	Polyvinyl Chloride
DTU	=	Delhi Technological University
MNRE	=	Ministry of New & Renewable Energy
COP	=	Conference of Parties
PSU	=	Public Sector Undertaking

Greek Symbols

η	=	Efficiency
ΔT	=	Temperature Difference
ρ	=	Density (kg m^{-3})
β	=	Thermal Expansion Coefficient
μ	=	Kinematic Viscosity
α	=	Thermal Diffusivity
k	=	Turbulent Kinetic Energy (TKE)
ε	=	Turbulent Dissipation Rate (TDR)

Subscripts

a	=	Ambient
o	=	Overall
out	=	Outlet
in	=	Inlet
coll	=	Collector
ch	=	Chimney
turb	=	Turbine

CHAPTER – 1

INTRODUCTION

Developing countries like India, China are heavily dependent on conventional sources of energy like coal, oil and gas to fulfill their growing energy needs. Continuous progress and development of the community requires motion and energy. Most of the developing countries import fuels as they are not in possession of energy resources and their population is exponentially increasing every few years and the ultimate result of which is civil wars and disputes with the neighbor countries. Fossil fuels have been the backbone of industrial development for almost the last two centuries and the use of which is still continuing. The fossil fuels are not only non-renewable sources of energy but they also have some unwanted side effects. The most common side effects include smog, acid rain, and global warming. The environmental pollution has reached such a high level that it is an alarming situation for wildlife, vegetation, and human health. The current consumption trend estimates that coal reserves will last only for some 250 years, oil for some 60 years and natural gas for approximately 80 years (Çengel & Boles, 2015). There can be two ways to combat such alarming situations, the first one is replacement of fossil fuels with renewable sources of energy and the other one is to aware the community to use the resources wisely keeping in mind the sustainable use of resources for the future generations as present generation has borrowed the resources from our upcoming generations. Energy efficiency is the judicious use of resources without compromising with the standard of living so that it ultimately results in energy conservation. The most common renewable sources of energy include solar energy, wind energy, hydro energy, biomass energy, and geothermal energy. Ocean energy, tidal energy, and wave energy are also considered as sources of renewable form of energy but much work has to be done to make these energies more affordable for the common people.

An energy source is renewable in nature if it can be renewed again and again without any significant reduction in its potential and no visible changes in the environment are observed. Renewable sources of energy can also be referred to as an alternative or green energy source as they do not harm the environment. On the

other hand, fossil fuels such as coal, oil, and gas are non-renewable sources of energy as they are depleted with consumption. The nature has provided us with a tremendous source of energy i.e. Sun. Energy from the sun is renewable which flows naturally and repeatedly. Sun is the ultimate source of energy because the origin of all other forms of energy is Sun except nuclear energy (Breeze, 2005) as shown in Fig. 1.1. Plants do photosynthesis processes in the presence of bright sunlight and release oxygen in the atmosphere which is essential for human life. Biomass is the organic plant matter created by the process of photosynthesis and hence, it is an indirect form of solar energy. For millions of years, this biomass remains buried under the earth's surface and resulted in the formation of fossil fuels like coal, petroleum, etc. which is again an indirect form of solar energy. Other indirect forms of solar energy include wind energy, wave energy, tidal energy, and ocean thermal energy.

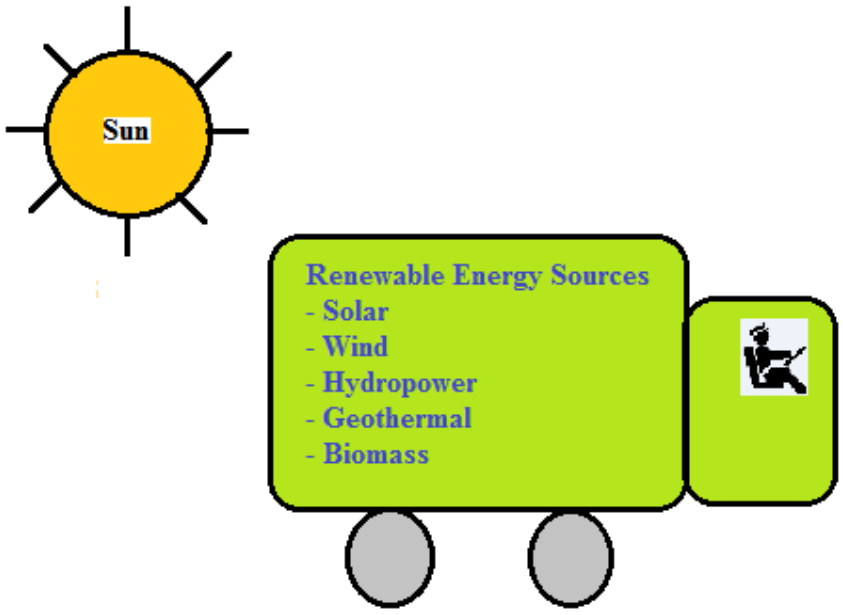

Fig. 1.1 Sun as the driver of all other forms of renewable energy

1.1 Solar Energy

The electromagnetic radiations emitted by the sun that reaches the earth's surface are called solar radiations or solar energy. The major advantage of solar energy is that it is the cleanest form of free energy available on earth with minimum running cost and is also non-polluting in nature. The energy flux received from the sun to the outer surface of the earth is 1373 W/m^2 (Çengel & Boles, 2015) and it is variable since the orbit of the earth on which earth revolves around the sun is elliptical. Hence, the mean distance between earth and sun varies and so does the value of Solar constant. The power of the sun intercepted by the earth is near about 1.7×10^{17} W (Çengel & Boles, 2015) and if one is able to harness this energy with even less than one percent efficiency then it would be sufficient for the world power consumption. The energy from the sun is required to keep the earth warm for life. The cost of harnessing solar energy is higher than that of the conventional sources of energy such as coal, oil or natural gas but it has more potential than the renewable sources such as wind, geothermal, hydro and biomass.

1.1.1 Merits of harnessing Solar Energy

1. Availability: The presence of a wide geographical area ensures sufficient availability of solar radiation.
2. Replenish-able: Solar energy is able to replenish continuously over a large time period.
3. Eco-friendly: Solar energy is one of the cleanest forms of available renewable sources of energy.
4. Cost: Running cost is minimal as there is hardly any rotating element and not much maintenance is required.

1.1.2 Demerits of harnessing Solar Energy

1. Solar energy is the dilute form of energy.
2. The extraction of useful forms of solar energy required a large land area.
3. Solar energy is a highly fluctuating form of energy which is dependent on geographical locations as well as the weather condition.
4. Initial investment is quite high for harnessing useful forms of solar energy.
5. The availability of solar energy is intermittent in nature.

1.1.3 Culp (1991) mentioned three utilization methods for the conversion of solar energy into other useful forms of energy.

1. **Helio-chemical method**: It is generally known as photosynthesis which results in the formation of biomass and fossil fuels. Fossil fuels are nothing but organic matter buried under the surface of earth for thousands of years.
2. **Helio-thermal method**: Using this method, the collected solar energy is converted into heat which can further be utilized for various applications like cooking, room heating, etc. Solar collectors and heliostats are normally used for capturing the heat from the sun.
3. **Helio-electrical method**: Using this method, solar energy is directly converted to electricity by the use of Photo-Voltaic (PV) or solar cells.

1.2 Solar Radiation

The sun is the primary source of energy. The power of the sun received by the earth's surface in the form of electromagnetic waves is about 1.8×10^{14} kW (Çengel & Boles, 2015). The sun is a large spherical body with a diameter of 1.39×10^{6} km and a mass of about 2×10^{30} kg (Çengel & Boles, 2015). The mean distance of the sun from the earth is about 1.5×10^{8} km. The energy is continuously formed due to the fusion reaction which took place in which two hydrogen atoms fuse together to form a helium atom. Therefore, the sun in nothing but a nuclear reactor. The temperature of the inside core of the sun is of the order of 10^{7} K while the temperature of the outer region of the sun is about 5800 K (Çengel & Boles, 2015). The amount of solar energy that reaches the earth's surface is known as solar irradiance or solar constant. The scientific community has adopted the value of solar constant as 1373 W/m^2 (Çengel & Boles, 2015). The value of solar constant is variable because the orbit of the earth on which earth revolves around the sun is elliptical in shape and therefore, the mean distance between the earth and sun varies and so does the value of solar constant. The variation in the value of the solar constant is about ±3.3%.

$$I_{sc}' = I_{sc}\{1+0.033\ \mathrm{Cos}\ (360\times\frac{n}{365})\} \quad (1)$$

where, I_{sc} = Solar constant value

n = n^{th} day

The maximum solar flux (1411.4 W/m^2) strikes the earth's surface on 21st December in the southern hemisphere whereas the minimum solar flux (1320.6 W/m^2) strikes the earth's surface on 21st June in Northern Hemisphere in perpendicular direction.

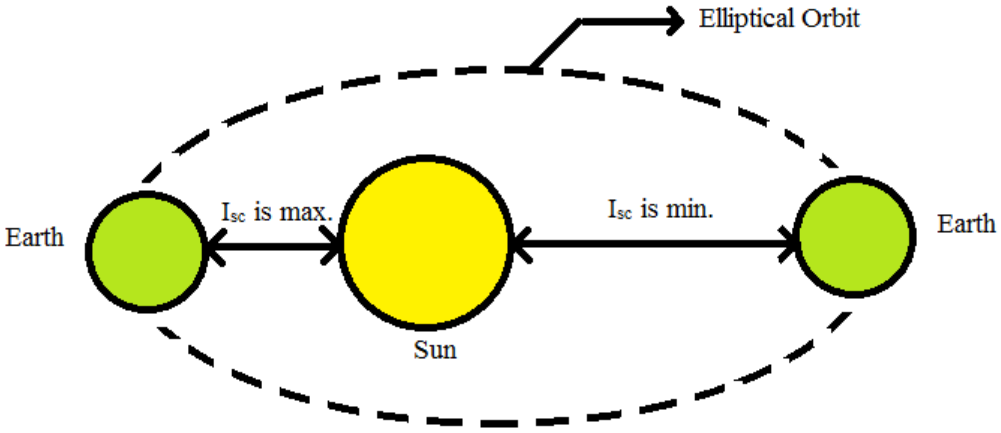

Fig. 1.2. Variation of Solar Constant

Earth is tilted at 23.5^0 with respect to its axis. Considering the Northern hemisphere, one can observe from the below figure that on 21st March and 21st September, the day and night are equal (Equinox). 21st June (Summer) is observed as the longest day in India and Earth is farthest from the Sun (Aphelion). Further, 21st December (Winter) is the shortest day observed in India and Earth is near to Sun (Perihelion).

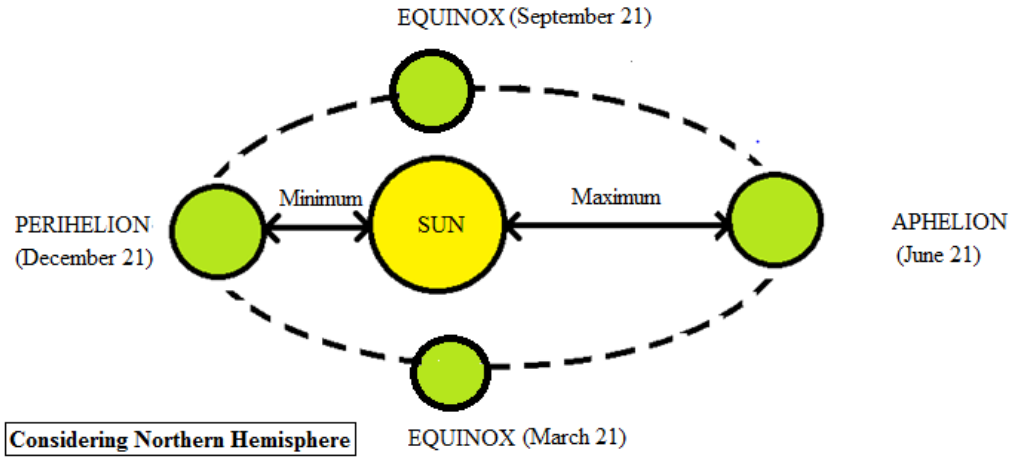

Fig. 1.3. Equinox, Aphelion and Perihelion

1.2.1 Angles involved in Solar Radiations

1. Latitude angle (ϕ): The latitude angle of a specific location (say P) is the angle made by the radius of the line joining the location 'P' and the center of the earth with projection of the line on the equatorial plane.
2. Longitude angle (L): Longitude angle is always measured from the reference point (Greenwich, England) and it is defined as the angle between the projection of the line of point 'P' on the equatorial plane and the projection of line with latitude of the reference point i.e. GMT line.

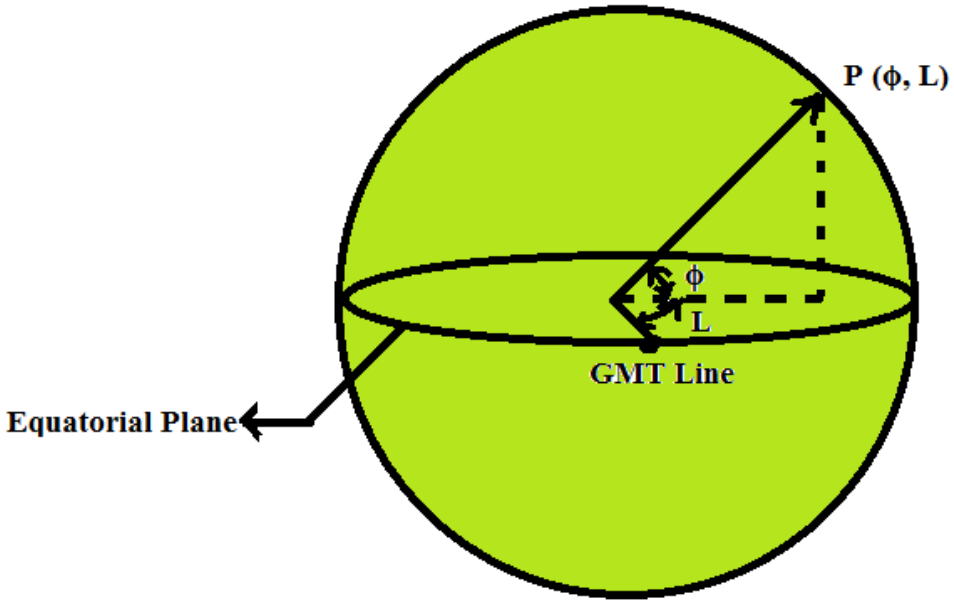

Fig. 1.4. Latitude and Longitude angle

1.2.2 Effect of Environment on Solar Radiations

Solar radiations received on the earth surface undergoes absorption, scattering, and reflection by the ozone layer and water vapors present in the atmosphere. Solar radiations received on the surface of the earth in line with the sun are known as Direct Solar Radiations whereas solar radiation received on the surface of the earth after getting scattered due to the atmosphere of the earth is known as Diffused or Indirect Solar Radiations. The summation of direct and diffused radiations together is known as Global Radiation.

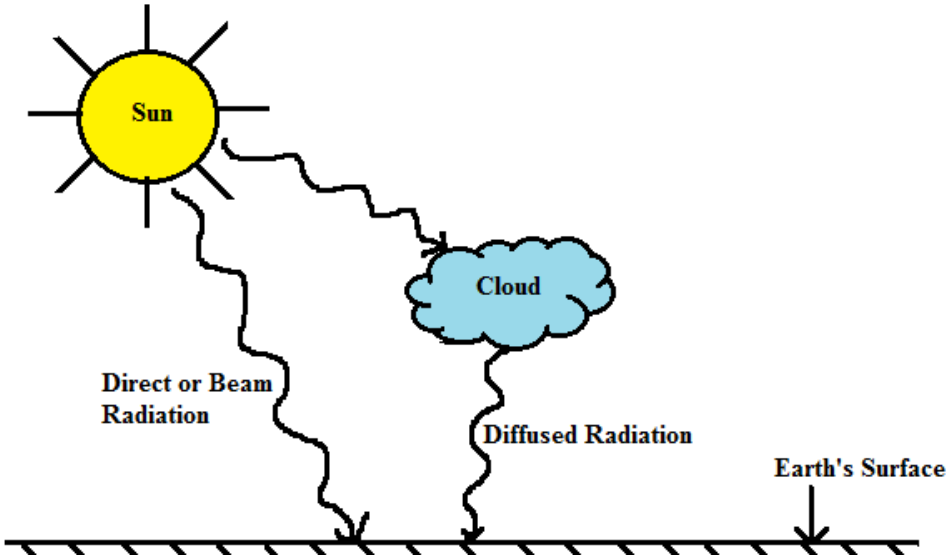

Fig. 1.5. Direct and diffused radiations

When solar radiations strike the surface of a material then some part of it gets absorbed, some part gets reflected while the rest part is transmitted through it. The summation of the solar radiation absorbed, reflected and transmitted is equal to the total solar radiation incident on the surface of the material.

$$\text{i.e. } \alpha + \rho + \tau = 1$$

where, α = Absorptivity

ρ = Reflectivity

τ = Transmissivity

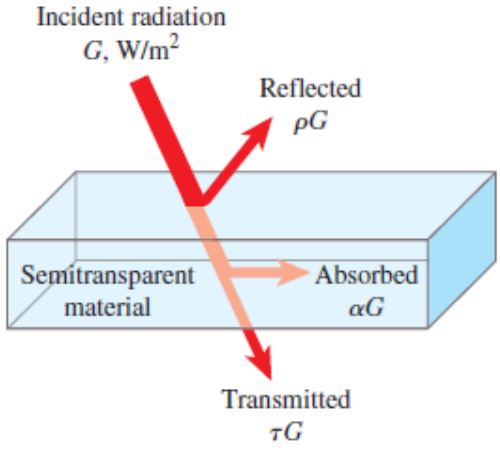

Fig. 1.6. Absorption, reflection and transmission of solar radiation through a surface (Cengel and Ghajar, 2011)

The value of emissivity for a black body is equal to 1. The value of emissivity for any surface varies in the range of 0 to 1.Surfaces that are meant for collecting solar radiation should have a higher value of α to collect the maximum amount of solar radiation and lower the value of ε to emit out less amount of solar radiation. In actual practice, the scientific community is more obsessed with α_s / ε ratio for selecting the material for heat absorption or heat rejection. For heat absorption higher values of α_s / ε ratio are preferred (galvanized sheet metal with α_s / ε ratio of 5.0) and for heat rejection lower values of α_s / ε ratio are preferred (anodized aluminum with α_s / ε ratio of 0.17).

1.3 Methods for capturing Solar Energy

Solar energy can be captured directly or indirectly. In direct methods, air or water is directly heated for the conversion of solar energy into electricity. A high energy fluid is made to expand into the turbine which loses its energy to generate shaft power. Concentrating type solar collector is used for energizing the fluid. Photovoltaic cells can also be used to directly convert solar energy into electrical power. In indirect methods, ecology systems are driven by solar energy. Wind and biomass energy are a few of the indirect methods. Biomass is an organic matter that includes all plants, vegetation, animals, and micro-organisms which are grown on land or water. Plants are developed by the process of photosynthesis process and energy is derived for photosynthesis by solar energy and therefore, considered as an indirect form of solar energy. In a similar manner, winds are created through unequal heating and cooling of the surface of sea, ocean or hills during the day and the night. Therefore, potential sites for harnessing wind energy are coastal areas and hilly areas. Hence, wind energy is also an indirect way to convert solar energy into electricity.

1.4 Devices for capturing Solar Energy

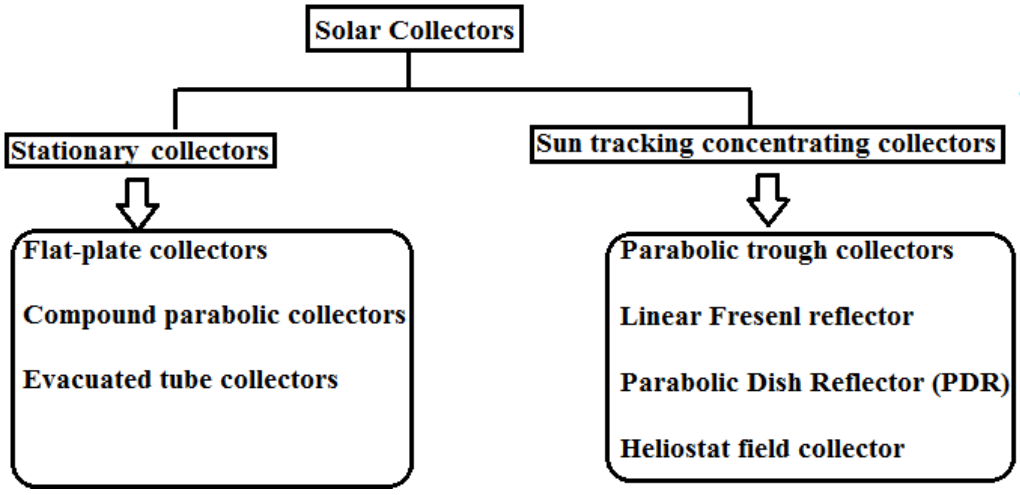

Fig. 1.7. Classification of devices for capturing solar energy

Devices for capturing solar energy exchange heat and converts solar heat energy to the internal energy of the fluid. The most essential equipment for the purpose of energizing the fluid is the solar collector. Solar energy collectors are basically considered of two types: concentrating and non-concentrating. A wide variety of solar energy collectors are available and some of the important collectors are mentioned in the table below.

Table 1.1

Solar Collectors and their specification (Kalogirou, 2004)

Type of Collector	Type of Motion	Concentration Ratio	Type of Application
Flat plate collectors (FPC)	Stationary	1	Low-Temperature Application
Evacuated tube collectors (ETC)	Stationary	1	
Compound parabolic collector (CPC)	Stationary	1 to 5	

Linear Fresnel reflector (LFR)	One-axis tracking	10 to 40	Medium Temperature Application
Parabolic trough collector (PTC)	One-axis tracking	15 to 45	
Cylindrical trough collector (CTC)	Double-axes tracking	10 to 50	High-Temperature Application
Parabolic dish reflector (PDR)	Double-axes tracking	100 to 1000	
Heliostat field collector (HFC)	Double-axes tracking	100 to 1500	

1.4.1 Stationary Collectors

These solar energy collectors are fixed and cannot locate the position of the sun. There are 3 types of solar energy collectors lying in this category.

1. Flat Plate Collectors (FPC)

   In flat plate collectors, solar radiation crosses through a transparent covering and strikes the absorber plat which has the ability to absorb large amounts of solar radiation. A good portion of this energy is carried away by the fluid-filled in tubes. The lower side of the absorber and sides of the casing are kept in isolation in order to minimize the heat dissipation. Tube carrying fluid can be made as a permanent joint with the absorbing plate or both can be extruded so as to become an integral part.

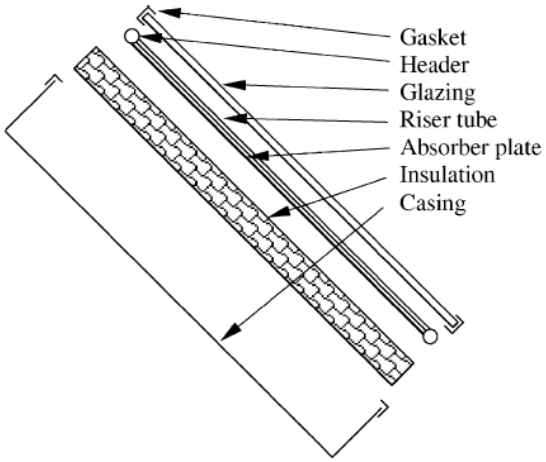

Fig. 1.8. Flat-plate solar collector (Kalogirou, 2004)

2. Compound Parabolic Collectors

The idea of parabolic collectors was conceptualized by Winston (Winston, 1974). Compound parabolic collectors consist of two portions of parabolic shape which face opposite to each other as shown in the Fig.11. Compound Parabolic Collectors have the capability to allow incoming solar energy radiations over a large variety of angles. Utilizing the principle of multiple internal reflection, solar radiation striking the collector in its range of acceptance angle is diverted to the absorber surface. Absorber surface can be cylindrical or flat.

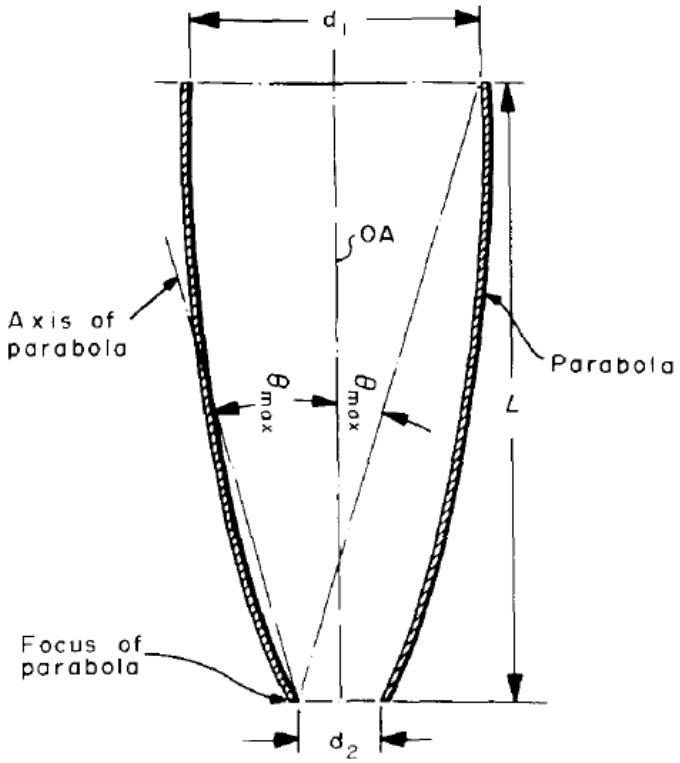

Fig. 1.9. Compound Parabolic Collector (Winston, 1974)

3. Evacuated Tube Collectors

In evacuated tube collectors, both direct and diffused solar radiations are utilized. ETC makes use of a phase change material (PCM). It consists of a heat pipe sealed inside a vacuum tube. The heat pipe contains some amount of methanol that periodically undergoes condensing and evaporating cycle. The

collector plate absorbs heat due to which the fluid inside the heat pipe (evaporator) absorbs heat and evaporates. This vapor form travels to the top where heat pipe (condenser) protrudes inside a manifold through which water or glycol flows and collects heat and supplies to another solar heat storage tank.

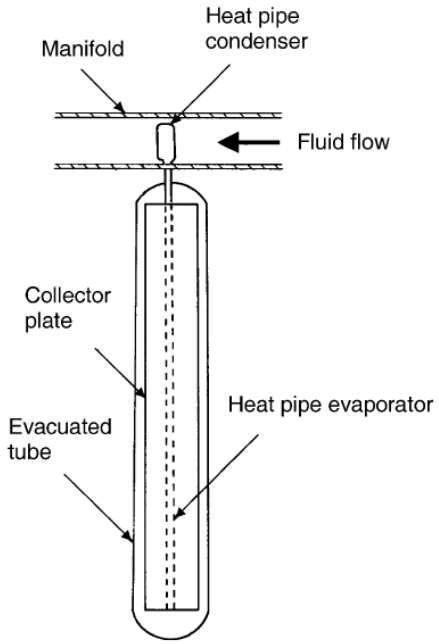

Fig. 1.10. Evacuated Tube Collector (Kalogirou, 2004)

1.4.2 Concentrating Collectors

Heat losses are directly proportional to the surface area exposed to the environment. Therefore, to reduce heat losses if somehow, one should be able to focus the solar energy at a point or a line then heat losses can be minimized significantly. Very high temperatures can be achieved is great amounts of solar energy is focused on a relatively minimal area. To continuously focus solar energy at a point or a line, some kind of tracking device is required which can continuously follow the position of the sun just like a sunflower.

The collector which fall under this category are:

1. Parabolic Trough Collectors

   These collectors are used for high-temperature applications ranging from 50 degrees Celsius to 400 degrees Celsius. A sheet of reflective material is bent into a parabolic shape for the formation of parabolic trough collectors. When the parabola faces the sun, the parallel rays incident on the collector is directly diverted towards the receiver tube. The receiver tube of parabolic trough is along a straight line. The receiver tube is covered with a glass to minimize the convection heat loss.

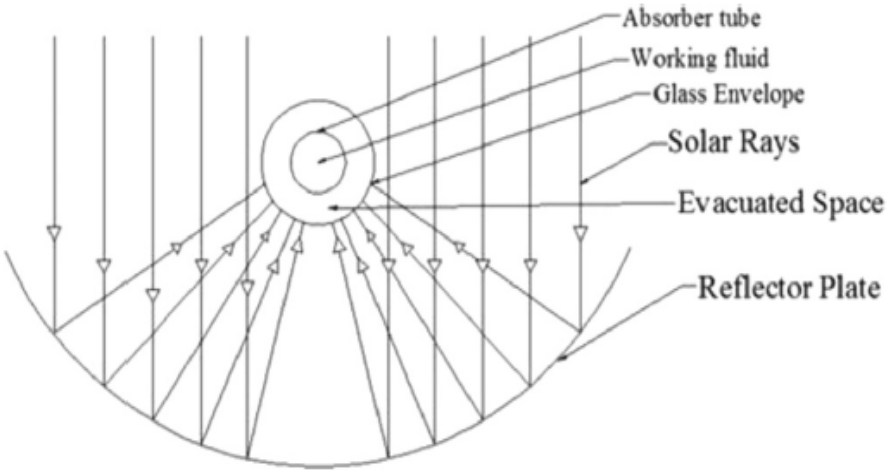

Fig. 1.11. Parabolic Trough Collector (Jebasingh & Herbert, 2016)

2. Linear Fresnel Reflector

   Linear Fresnel reflector is an arrangement of mirror strips placed on the ground so as to focus light on a single fixed acceptor which is placed at the top of a tower at certain height from the ground. Linear Fresnel Reflector can be considered as broken pieces of PTC but it is not of a parabolic shape. The flat reflectors makes this arrangement cheaper than the parabolic trough collectors. Also, the receiver is placed at a lesser height from the ground and therefore, the cost of erecting a structure is minimized. One problem with LFR arrangement is because of blockage and shade between neighbor fresenel reflectors, the distance between them has to be significant.

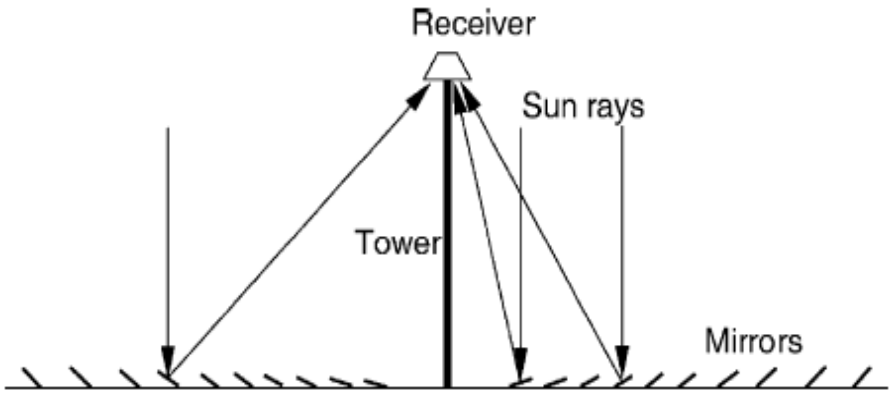

Fig. 1.12. Linear Fresnel Reflector (Kalogirou, 2004)

3. Parabolic Dish Reflector

   A parabolic dish reflector is similar to a dish antenna and is a point focusing collector that locates the position of the sun using a double axed tracking mechanism. The collector of this type is used for high-temperature applications and temperature as high as 1500 degrees Celsius can be achieved. The receiver absorbs the incident solar radiation and energizes the circulating fluid. Parabolic dish reflectors have a higher concentration ration and therefore, are highly efficient. It is commonly used in parabolic dish engines. In parabolic dish engines, fossil fuel is replaced with sunlight to generate electricity.

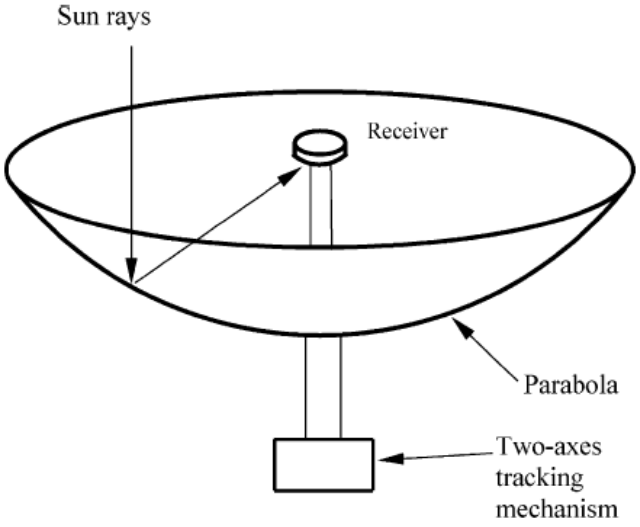

Fig. 1.13. Parabolic Dish Reflector (Kalogirou, 2004)

4. Heliostat Field Collector

Heliostats are nothing but an arrangement of flat mirrors. Heliostats are used for the very high requirement of solar radiation energy. Heliostats have the capability to direct the incident solar radiation towards a common receiver. It can be used to generate steam at a very high temperature and pressure. The concentration ratio is found to be in the range of 300 to 1500 and therefore, is highly efficient in collecting energy. The heliostats have reflective surface areas in the range of 50 square meters to 150 square meters. The heliostats reflect the solar energy directly onto the receiver which collects the solar energy and transfers this energy to energize the fluid. A solar thermal energy storage system collects the sensible part of heat and stores it for future usage. The average value of solar flux that strikes the receiver varies from 200 kW/m^2 to 1000 kW/m^2. This high value of flux allows the system to reach a high temperature of up to 1500-degree Celsius. The temperature requirement for the Brayton cycle is more than that of the Rankine cycle.

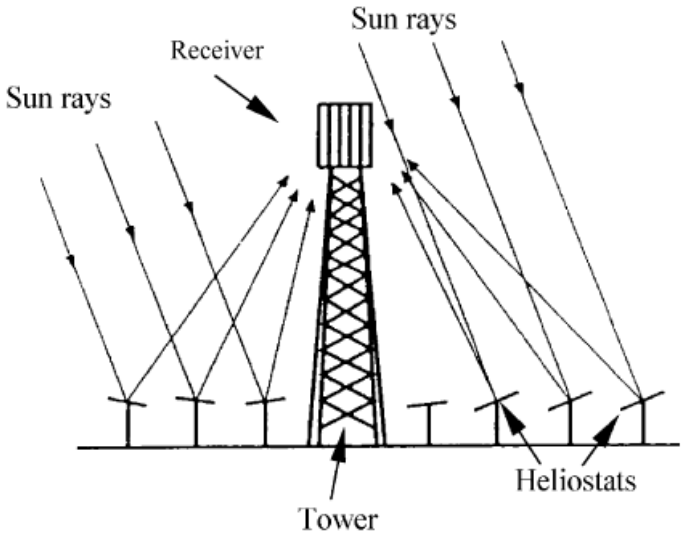

Fig. 1.14. Heliostat with central receiver arrangement (Kalogirou, 2004)

1.5 Photovoltaic Conversion of Solar Energy

The direct conversion of solar energy into electrical energy is known as solar photovoltaic conversion and the device used for this purpose is known as solar cell or PV cells. Solar cells are made up of semiconductor materials generally of crystal silicon in which n-type and p-type semiconductors fuse together by diffusion process.

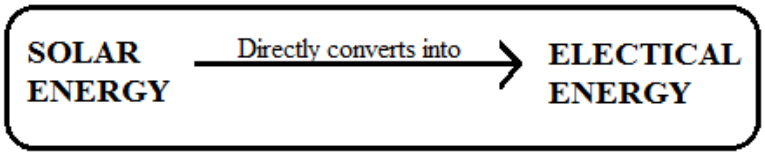

Fig. 1.15. Solar PV conversion

A thin layer of n-type semiconductor (about 0.25 micrometers) is diffused over a thick layer p-type semiconductor (about250 micrometers). Normally the front contact is made up of sintered glass and electrode consisting of 70% percent silver as an organic binder and an anti-reflective coating of Titanium dioxide is also provided over the top of the surface to increase the absorptivity.

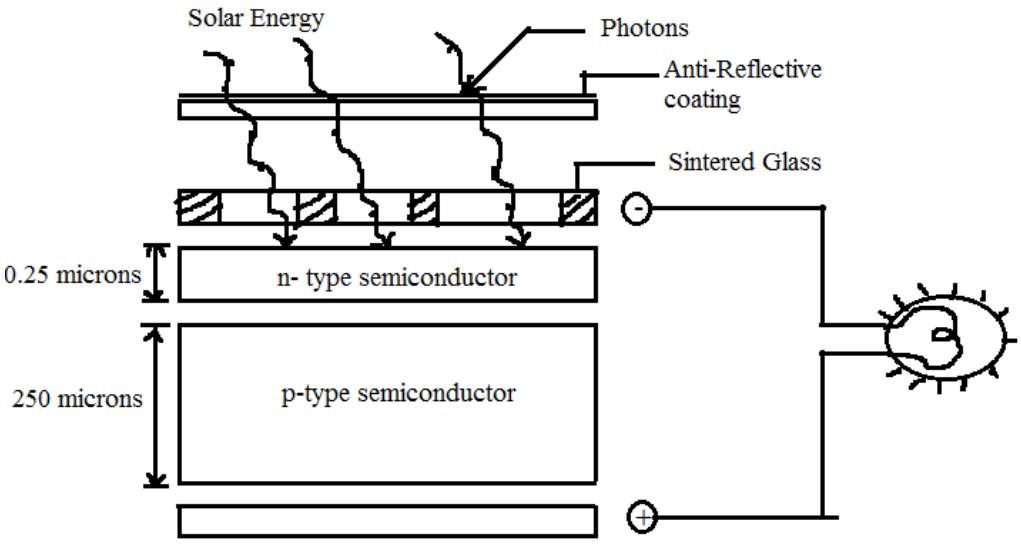

Fig. 1.16. Construction details of PV cell

In semiconductors, electron either occupies the valence band or the conduction band. The valence band is at a low energy level and completely occupied while the conduction band is at a high energy level and partially occupied. Energy associated with the band gap is the difference of minimum energy of the electron and the maximum energy of the electron in the conduction band and valence band respectively. When the cells are exposed to solar radiations, then the photons of the sunlight contain packets of energy and if this energy content is greater than the Band Gap Energy, then it excites some of the electrons and they are made to flow through an external circuit and thus producing electrical energy.

1.6 Solar Power Chimney (also known as Solar Updraft Tower)

To fulfill the energy demands of a growing economy, a promising technology like Solar Updraft Tower power plants which majorly is a combination of solar energy collector, vertical chimney or tower and a turbine. SUT technology makes use of incident solar radiations (INSOLATION) to heat up the air under the shelter created by a translucent solar collector and thus energizing the air which drives a vertical axis turbine located at the center of vertical chimney or tower to generate electricity.

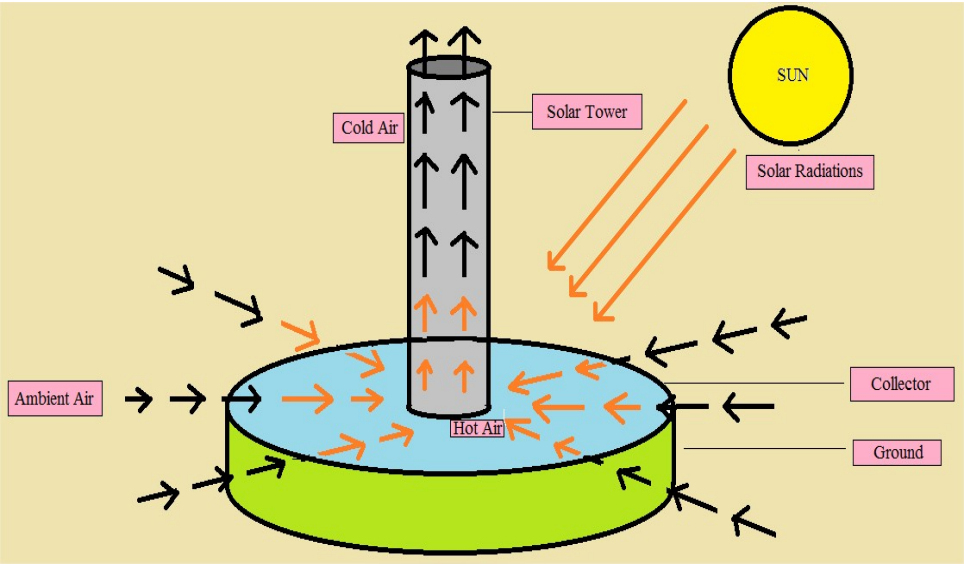

Fig. 1.17. Schematic Diagram of Solar Chimney Power Plant

Solar Chimney Power Plant has mainly three important components:

a. The Tower or Chimney

The tower can be considered as equivalent to a thermal heat engine SCPP as it converts heat into mechanical energy. The updraft effect is created due to the rising of hot air having low density. A decent volume flow rate and high strength of hot air is required for creating a strong updraft effect. To achieve these conditions, the plants must have a considerable amount of density difference of air between base & top of chimney.

b. The Solar Energy Collector

Collector captures both direct and diffused radiations available from the sun and heats up the air under it. It is the most common observation that when air gets heated up it becomes light in weight and thus tries to move upwards. The air entering at the collector inlet gets heated up during its path of travel s tarting from collector inlet to the tower inlet and thus creating a natural updraft because of the density difference. Heat losses from the collector should be as low as possible.

c. The Turbine

The difference of density between the atmospheric air and the air inside the collector creates a buoyancy effect which acts as a driving force for the air and is generally known as pressure potential. Because of the buoyancy effect air is allowed to flow inside the collector and rise in upwards direction in the vertical tower. The air while passing through the turbine blades loses its energy to the turbine to run & generate electricity utilizing a generator. The turbine utilized in the solar chimney power plant is similar to axial flow turbine i.e. Kaplan turbine used in the hydroelectric power plants.

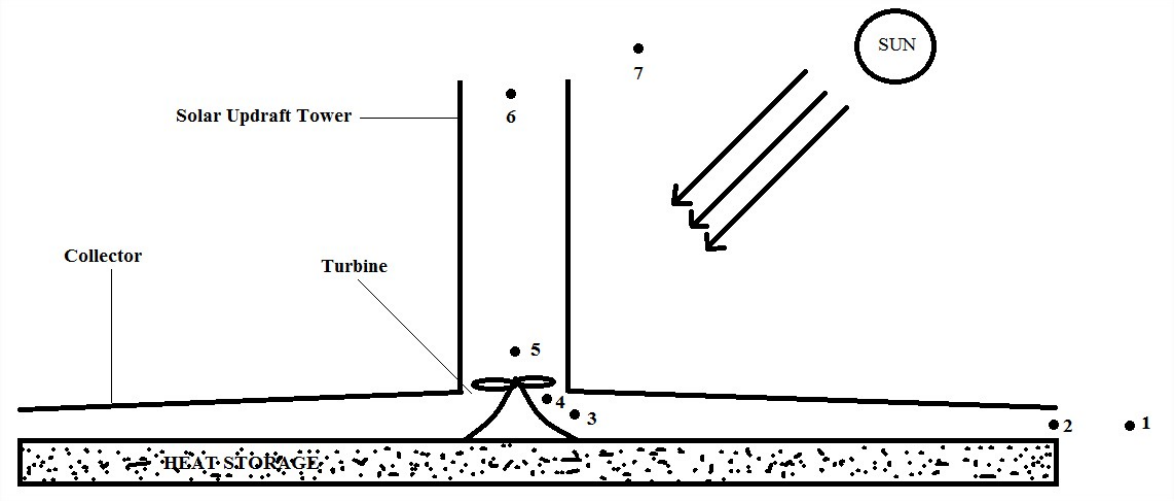

Fig. 1.18. Schematic diagram of conventional solar chimney power plant

As shown in the fig.1.18 following numbers indicate

1. Atmospheric air at bottom
2. Collector entry
3. Collector exit
4. Turbine entry
5. Turbine exit
6. Tower exit
7. Ambient air (tower outlet)

1.6.1 Historical improvements in solar updraft tower technology

The following historical improvements in the field of solar updraft tower technology have been clubbed together from Wikipedia (Wikipedia Contirbutors, 2018):

- In 1896, Mr. Alfred Rosling Bennett described a Convection mill and published the first patent for the same.
- In 1903 Isidoro Cabanyes, a spanish arm colonel suggested a solar chimney power plant in the magazine named La Energia Electrica and the same was described again in the year 1931 in a publication by a German author named Hanns Gunther.
- In 1982, Jorg along with his friends built the first ever experimental model of solar updraft tower in Manzanares, Spain. The pilot project tower of 194.6 m height and collector of 244 m diameter. The prototype was operational for 7

consecutive years starting from year 1982 to year 1989 (Schlaich J. , 1995) with a maximum output of 50 kilo Watts. The success of the model presented a feasible & reliable technology for power generation. Since then many scholars & researchers have inclined towards doing research in this technology and worked on to identify its potential on a large scale all over the world. Many commercial projects of solar updraft towers have been put forward in various parts of the world but still, the technology is not suitable for commercial use.

- In 2010, China's first solar chimney plant started operating in the desert in Mongolia. The plant claimed maximum power output of 200 kW.
- Since 2001, an organization named Enviro-mission has been improving and working to improve solar updraft tower technology.

1.6.2 Operational Principle

The energy conversion process in SUTPP can be represented with the help of the T-S diagram irrespective of losses as shown in Fig. 1.19. The working cycle of Solar Chimney power plant has so many similarities with the Brayton cycle used in the Gas Turbines

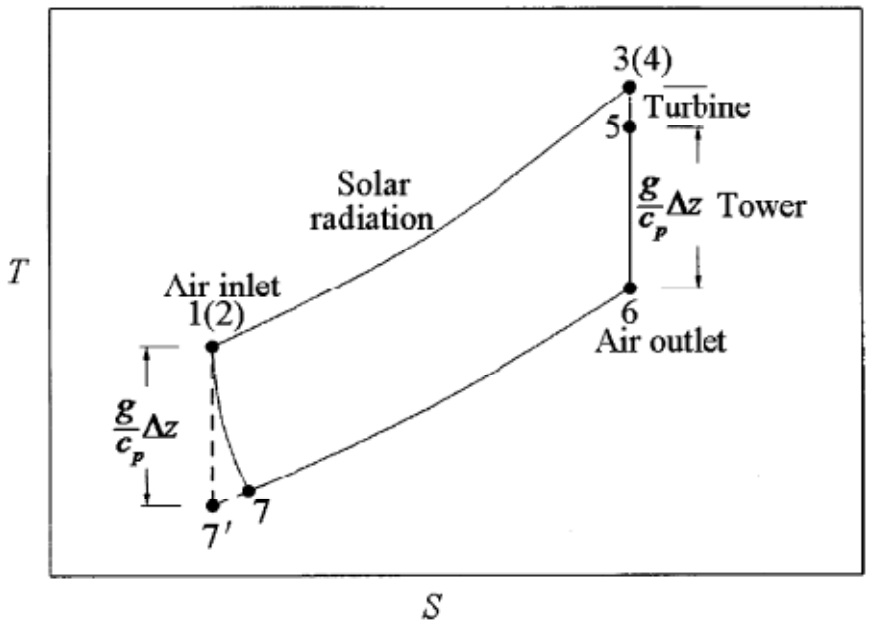

Fig. 1.19. T - s diagram irrespective of losses (Gannon & Backström, 2003)

1.6.3 Merits of Solar Power Chimney:

1. In a tropical country like India, Solar power chimneys are the best way to utilize both global and diffused solar energy radiations.
2. It can readily solve the problem of intermittent power supply conditions associated with the use of solar energy. Water filled tubes can be used as a storage medium to store heat since water has a higher value of C_p. Stored heat is released during the night to heat up the air and thus plant can be in operation full day.
3. There are no moving parts in the plant except the turbine and hence the maintenance cost of the plant is less.
4. Since there is no fuel requirement like in a conventional thermal power plant (coal is used as a fuel) and therefore, results in lower operating costs.
5. Construction requires easily available material like concrete and glass.
6. Construction of such huge chimney structure require labors in huge number and hence will create a good number of jobs in the region.

1.6.4 Demerits of Solar Power Chimney:

1. The efficiency of solar power chimney is poor but the use of cheap material, robust construction & low maintenance cost compensates for the same.
2. It requires a large land area. Deserted areas that are uninhabitable for the human race can be utilized.

1.6.5 World's First-Ever Prototype – Manzanares, Spain

Based on years of research and numerous wind tunnel experiments under the guidance of Schlaich and Bergermann, the world's first-ever solar updraft tower was designed, constructed and operated with a maximum power output of 50 kW in Manzanares, Spain. The pilot prototype has a tower of 194.6 m height and a solar collector of 122 m in radius (Haaf, Friedrich, Mayr, & Schlaich, 1983).

Fig. 1.20. Manzanares Prototype (Haaf, Friedrich, Mayr, & Schlaich, 1983)

The roof the collector should be translucent, withstand extreme weather conditions and cost should be reasonable. Different types of plastic sheets and glass were selected to find the suitability for the weather conditions and cost. It was found that glass could resist harsh storm conditions without harming and are self-cleaning in nature because of the occasional rain drizzles.

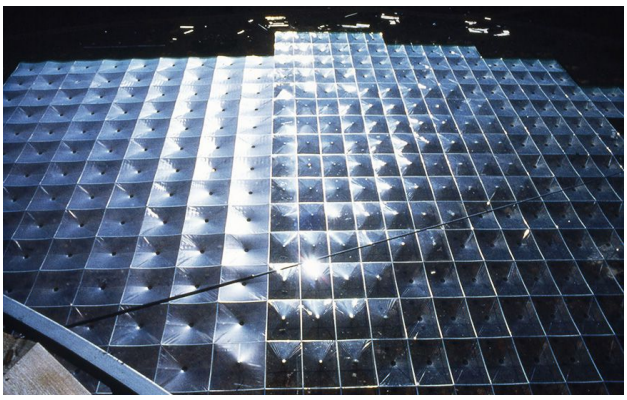

Fig. 1.21. Collector Roof (Schlaich & Bergermann, 2018)

The turbine was supported independently over a steel structure. During the startup 2.5 m/s velocity was observed reaching a maximum up to 8 m/s (Haaf, Friedrich, Mayr, & Schlaich, 1983). The tower consisted of a guyed tube of trapezoidal sheets. The tower tube stands were supported on ring which was 10 m above the ground level.

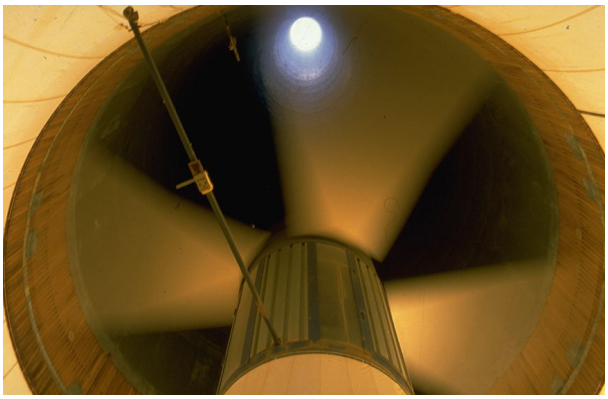

Fig. 1.22. Wind Turbine (Schlaich & Bergermann, 2018)

In the year 1987, the plant was operational for a total of 3197 hours operating closely to 9 hrs a day. The plant started up automatically as soon as the air flow velocity reaches up to 2.5 m/s. Results reflected that the system and its components were in synchronization with each other (Haaf, Friedrich, Mayr, & Schlaich, 1983).

CHAPTER - 2

LITERATURE SURVEY & REVIEW

Schlaich & Schiel (2003) described how several wind tunnel experiments led to the existence of first-ever SUTPP in Manzanares, Spain. Construction of the prototype was completed in 1982. The main motive of the plant was to present the working principle of solar chimney along with demonstrating its fully automatic behavior and efficiency. The plant could produce a peak power output of 50 kW. The plant starts automatically as soon as the air velocity of 2.5 m/sec is attained. While passing through the collector air temperature rises up by 17 K and maximum air velocity of 12 m/sec was achieved. Collector roof and chimney have been referred to as analogous to reservoir and penstock respectively of hydroelectric power plant.

Zhou et. al. (2007) experimentally investigated the temperature field of solar chimney power setup. The geometrical dimension of the setup includes a collector diameter, chimney height, chimney diameter, height from ground to collector outlet and height from ground to collector inlet of 10 m, 8 m, 0.3 m, 0.8 m and 0.05 m respectively It was the first attempt to perform an advance study of the temperature fields of solar chimney power plant systems. Maximum incident radiations are possible only when the slope of the collector is equal to the local latitude of the location. However, due to manufacturing constraints, the actual slope was considered as 8^0 but ideally should be 30^0 according to the geographical location. After the analysis of temperature distribution, it was found that there appears a temperature inversion during the dawn time due to continuously increasing solar radiations & vanishes once the air beneath the collector is heated to a sufficiently higher temperature generating an upward thrust which is powerful enough to destroy the temperature inversion layer and allows the air to flow out through the chimney.

Zhou et. al. (2009) proposed a unique and novel concept to integrate solar collector with a mountain. Mountains can be excavated and made hollow to avoid the safety

issues arising out of erecting a gigantic reinforce concrete structured chimney. The conversion of this thought into reality will result in the saving of construction materials. Such a power plant can be made in the countries in which there are unused mountains and plateaus. In this way, every mountain will serve as a power plant. Driving force to drive the turbine is proportional to the height of chimney but erecting such huge structures requires advanced technical expertise along with years of experience. Also, there is a limit to erect structures of such a height as there are some technical constraints but hollow mountains can serve the same role as that of a chimney without worrying about the safety issues.

Zhou et. al. (2010) evaluated the performance of solar power chimney in Qinghai-Tibet plateau using simple mathematical model. Availability of vast barren land, an abundance of direct solar radiations, low atmospheric temperature and availability of a number of salt lakes make Qinghai-Tibet plateau an ideal place. Salt lakes in the plateau region can be used as heat storage for delivering power during the night time. Power output increases with the increase in the dimension of the chimney and collector area. An increase in solar radiation also enhances the performance of the plant. The increase of ambient temperature during the day time affects the performance but higher ambient temperature is beneficial for the power output during the night. With greater amount of solar radiation, the power output of the solar power chimney plant in Qinghai-Tibet plateau is more than that of the same latitude regions which are not part of the plateau. Plant was expected to power the rail transport and support agenda of development along with other renewable energy sources.

Zhou et. al. (2013) tried to predict the potential power that could be produced from the SCSUTPP. The use of a sloped collector will help to increase global & diffused radiations received by the solar collector and simultaneously results in a decreasing incidence angle. The basic design of sloped solar collector presented based on a mathematical model that is suitable for both the conventional horizontal collector SUTPP. A proposed 5 MW plant in Ottawa is the basis of the design of a sloped collector SUTPP and two horizontal collector SUTPP. It was concluded that

building a sloped collector can eliminate the cost of erecting huge SUT structures. As part of the economic analysis, one has to decide whether to opt for the construction of SCSUTPP or HCSUTPP as selecting the former will result in savings of construction cost of SUT and selecting the latter will result in savings of construction cost which include leveling off uneven surface along the mountains, cost of transportation and so on.

Kalash et. al (2013) experimentally investigated the temperature field of a sloped solar collector updraft power plant on the campus at Damascus University, Syria. The location for the experimental setup was carefully selected so that there are no shading obstructions. The collector had a triangular shape with a tilt angle of 35^0 towards the south. The total collector area is about 12.5 m^2. The chimney was 9m tall with diameter of 0.31m.The temperature measurements were continuously monitored every 10 minutes for continuous 40 days during winters for the performance evaluation. A total of 18 Platinum resistance thermocouples were utilized to record the temperature. Even though the experiment was carried out in winter season, the maximum temperature between the chimney inlet and the ambient was observed to be 19^0C with an updraft air velocity of 2.9 m/s in the chimney. Solar radiation is directly linked with the chimney inlet temperature. Also, it is evident that there is an association between ambient temperature and chimney inlet temperature but the effect of ambient temperature on chimney inlet temperature is minimum during noontime. As the radiations starts to decrease, soil starts emitting the stored heat. To realize the actual conditions, the soil from the mountains in Syria was used in the experiment and soil storage capacity was good enough to keep the temperature fixed.

Kalash et. al. (2014) conducted experiment on the sloped solar updraft tower setup in the mechanical engineering department of Damascus University and data was collected every 10 minutes for a complete year between December 2011 to November 2012. The average values of collector outlet, chimney inlet and ambient temperature for each month were collected using a data acquisition system setup in a room above which tower was supported.

Xu & Zhou (2018) studied the effect of altering chimney outlet and inlet area on various parameter which include Total Pressure Potential (TPP), Collector Temperature Rise (CTR). Selecting large value of COAR will result in separation of boundary layer, flow stalling, backflow & formation of vortices. The flow area is also blocked and becomes large with an increase in chimney height. On increasing value of COAR, the TPP first shows increasing nature and decreases beyond COAR value of 8.7. Even before the flow stall occurs EPPRC decreases at a slower rate but after the flow stall has occurred EPPRC shows a sharply decreasing nature.

Hassan et. al. (2018) numerically investigated the performance of SCPP by varying diverging angles of chimney and slope of the collector. CFD simulation results were validated by comparing it with the experimental results and data of the Manzanares prototype. Chimney diverging angle of 1^0-3^0 and collector slope of 4^0, 6^o, 8^o and 10^o were considered for performing numerical simulations. Increasing slope of Collector beyond 6^0 results in non-uniform flow of air, air recirculation and formation of vortices. By keeping diverging angle as 1^0, there is a velocity increment from 9.1 m/s to a maximum of 11.6 m/s which increases the power output by 108%.

Najm & Shaaban (2018) tried to investigate the optimum collector radius, efficiency and power density based on the available incident solar radiations. Collector radius of 32-172 m, 32-400 m and 72 m were chosen for the study. Chimney height with varying dimensions 175 m, 185 m, 195 m, 205 m, 215 m were numerically investigated for the optimization of the performance. Various irradiance conditions were considered such as 300 W/m^2, 400 W/m^2, 500 W/m^2, 700 W/m^2 and 900 W/m^2. Ambient temperatures under which simulation were performed include 293-323 K and 300 K.

Fadaei et. al. (2018) experimentally investigated the solar power chimney with and without the use of Phase Change Materials (PCM). Paraffin wax was used as a PCM. During day time paraffin wax stores latent heat and gets converted into a liquid phase and during the night time, it releases latent heat and changes into a solid

phase in the absence of sunlight. The geometrical dimension of the experimental model includes chimney height, collector diameter, collector height and a chimney radius of 3 m, 3 m, 0.06 m and 0.10 m respectively. Overall increase in thermal efficiency was observed.

Fathi et. al. (2018) presented the idea to combine the nuclear power plant and SCPP for improving the efficiency of the combined cycle power plant by utilizing waste heat from the nuclear power plant. The basic idea was to make use of the waste heat from nuclear power plants and replacing wet cooling towers with a dry cooling tower (i.e. Solar chimney power plant). Geometric dimensions same as that of the Manzanares prototype was used for the study. It was found that the total thermal efficiency of the combined cycle can be increased by 8.7%. It can be concluded that the combined cycle system is more preferable for the arid environment where there is a scarcity of water like desert areas.

Eryener & Kuscu (2018) presented the idea of hybridization of transpired solar collector and photovoltaic panels in a solar updraft tower using an experimental setup. The geometric parameter includes tower height, tower diameter, outer roof height and inner roof height. of 16.5 m, 0.96 m , 0.5 m and 1.5m respectively. The total area of the collectors including transpired solar collector and polycarbonate area was 314 square meters. There were total 28 number of photovoltaic panels with 264 W of power per module and thus, total photovoltaic power came out to be 7420 W. Rotor diameter of turbine was 0.8 m and was able to produce 200 Watt power. The slope was kept at 4^0. The solar power conversion efficiencies of the hybrid solar updraft tower are between 16 to 18 percent. The solar collector area can be significantly reduced with the increased solar conversion efficiency and thus making it, even more, cost-effective.

Amudam & Chandramohan (2019) compared two 3D models of solar updraft tower – one with considering thermal energy storage and another without considering storage. Sand rock mixture of thickness about 0.15 m was used as heat storage material. Geometric dimensions of the model include a collector diameter, chimney height and inlet gap of 3.5 m, 6 m & 0.15 m respectively. Slope of the collector was

taken as 30^0. Flow parameters such as temperature, velocity, pressure, and density were studied. Power output, collector efficiency, and overall efficiency were considered as performance parameters. 3D model of solar updraft towers that were solved using the Discrete Ordinate model along with the use of Solar ray tracing is very rare. Based on Bernoulli's principle, pressure has decreasing nature for both the models considered for the study. The maximum velocity achieved for the model with and without thermal energy storage was 4.24 m/s and 6.8 m/s respectively and the maximum temperatures with and without use of storage were found to be 306.5 K and 308.5 K respectively. Also, the maximum power developed with and without the use of storage were 63.8 W and 79.92 W respectively.

Jafarifar et. al. (2019) developed a 3D model of solar updraft tower and performed numerical simulations in ANSYS fluent to get the suction effect of the atmospheric winds and the same suction effect was applied to 2D model with axis-symmetric shape. Treating the Manzanares prototype as an ideal prototype, results were compared with it. Geometric dimensions include tower height, collector radius, tower radius, collector inlet height, collector slope and collector/tower fillet radius of 202 m , 120 m, 5 m, 2 m, 5^0 and 10 m respectively. Based on the results of the numerical study, it was concluded that winds may enhance the efficiency of a solar updraft tower by about 15% even in low solar radiation conditions.

CHAPTER - 3

EXPERIMENTAL SETUP, INSTRUMENTATION & METHODOLOGY

3.1 Experimental Setup

Fig. 3.1. Experimental model of Solar Power Chimney

The experimental setup as shown in the Fig. 3.1 consists of the following essential components:

3.1.1 Solar Power Chimney: The material for Solar Power Chimney is selected as Mild Steel for the ease of rolling into a cylindrical shape of outside diameter of 207 mm and length of 950 mm. The thickness of the MS sheet is 1 mm. The tower is painted black so as to absorb maximum solar radiations (absorptivity of black paint is 0.97).

3.1.2 Collector: The collector is made of a PVC sheet of 1 mm thickness to produce a greenhouse effect under the collector. The collector chosen is a sloped collector with a latitude angle of about 28.75^{o}. The lateral or curved surface area of the collector is about 1.5895 m^2.

3.1.3 Turbine: For the experimental setup inline duct fan with 6 blades and a diameter of 6 inches is being utilized to play the role of axial flow wind turbine. The inline duct fan is rated at RPM of about 3000 which is practically required for electricity generation.

Table 3.1

Dimensions of the experimental setup of Solar Power Chimney

Chimney height	0.95 m
Chimney diameter	0.207 m
Collector height at entry	0.2 m
Collector height at exit	0.5 m
Collector area	1.5895 m^2

Fig. 3.2. Some photos clicked during manufacturing of experimental model

3.2 Instruments Used

The instruments used for the experimental analysis have been incorporated in the Table 3. The instruments includes solar power meter, anemometer, thermal-hygrometer, tachometer, multi-meter, thermocouple cable and temperature indicator.

Table 3.2

Instruments used for recording observations

S.No.	Item Description	Purpose	Specification
1.	Solar Power Meter	To measure Global and Diffused radiations at the collector	Silicon photodiode sensor
2.	Anemometer	To measure the air velocity at various locations	Range: 0.6 to 40 m/s
3.	Thermal hygrometer	To measure the Relative Humidity	Range: 0 to 50 degree Celsius
4.	Tachometer	To record the RPM of the inline duct fan	Range: +1 to +99999 rpm
5.	Multi-meter	To record the Voltage and Current output of the inline duct fan	True RMS measurement
6.	Thermocouple cable	To be utilized for recording surface temperature along with temperature indicator along at various locations	K-type Teflon Cable
7.	Temperature Indicator	To record temperature readings at various locations	Input: K type

3.3 Experimental Uncertainty Analysis

The experimental percentage of uncertainty has been considered for the temperature parameter since it is quite sensitive. Experimental uncertainty percentage is the sum total of internal and external uncertainty percentage. External uncertainty percentage

is considered as the least count of the measuring instrument while the internal uncertainty percentage is calculated as follows (Chauhan & Kumar, 2017):

$$\text{Internal Uncertainty \%} = \frac{U}{\text{mean of total observation}} \times 100 \quad (2)$$

Internal uncertainty (U) is determined as below

$$U = \frac{\sqrt{\sigma_1{}^2 + \sigma_2{}^2 + \sigma_3{}^2 + \cdots + \sigma_n{}^2}}{N} \quad (3)$$

Where σ = Standard Deviation and is calculated as

$$\sigma = \sqrt{\frac{\sum(X - \bar{X})^2}{N_0}} \quad (4)$$

where,

$(X - \overline{X})$ = Deviation from the average value

N = Total number of sets and

N_0 = Number of observations in each set..

Table 3.3

Experimental uncertainty % considering sensitive parameter like temperature

S.No.	Observed Parameter	Total uncertainty (%)		
		Int.	Ext.	Total
1.	Ambient Temp.	0.0923	0.1	0.1923
2.	Temp. Inside Collector	0.1028	0.1	0.2028

3.4 Methodology

3.4.1 Experimental Analysis

An experimental model was setup at the roof the Mechanical Engineering Department of Delhi Technological University (Delhi, India) to analyze the performance of the Solar Power Chimney for three days starting from September 10, 2019 to September 12, 2019. Dimensions for the 3D model of the setup was chosen based on the space constraints and the ease of manufacturing. SOLIDWORKS was used to create the physical domains of the experimental model. A chimney height of 0.95 m, chimney diameter of 0.207 m, collector height at entry & exit of 0.2 m & 0.5 m respectively were taken into consideration as the dimensions of solar power chimney and slope of the collector was chosen as 28.7501^{o} considering the geographical location of DTU, Delhi (latitude 28.7501^{O} N &longitude 77.1177^{O} E). The readings were recorded using the various instruments listed for a total of three days starting in the morning at 8:00 AM to evening 6:00 PM at an interval of every one hour.

The parameters for performance evaluation of the experimental setup of Solar Power Chimney have been described here.

The collector efficiency as suggested by (Zhou & Xu, 2016)can be estimated using the following equation:

$$\eta_{coll} = \frac{\dot{m}\, c_p(T_{out} - T_{in})}{I_g \times A_c}$$

Upon neglecting the aerodynamic losses, the Solar Power Chimney efficiency can be derived using the given equation (Nizetic & Klarin, 2010):

$$\eta_{SUT} = \frac{gH}{C_p T_a}$$

The overall efficiency of the Solar Power Chimney power plant can be determined using the equation:

$$\eta_o = \eta_{coll} \times \eta_{ch} \times \eta_{turb}$$

The turbine efficiency is assumed as 80 percent for small plants of 30 MW in most of the literature and therefore, it is a reasonsniable assumption to assume turbine efficiency as 80 percent for the experimental setup (Schlaich J. , 1995)

The electrical power output of the Solar Power Chimney power plant can be calculated using the equation:

$$P = V \times I$$

Thus, overall thermal efficiency can also be represented as:

$$\eta_o = \frac{VI}{I_g \times A_{coll}}$$

The mass flow rate is calculated using the following continuity equation by assuming one dimensional steady flow:

$$\dot{m} = \rho A v$$

where v is the velocity (in m/s) entering the collector

The area of the collector can be calculated by assuming it as the curved surface area of the frustum of the cone:

$$A = \pi(R + r)s$$

where s is the slant height of the collector

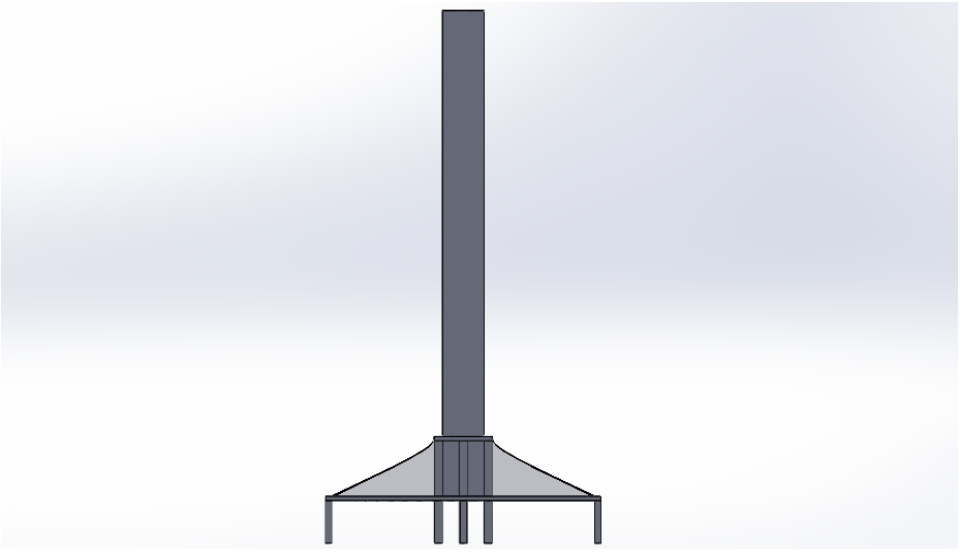

(a)

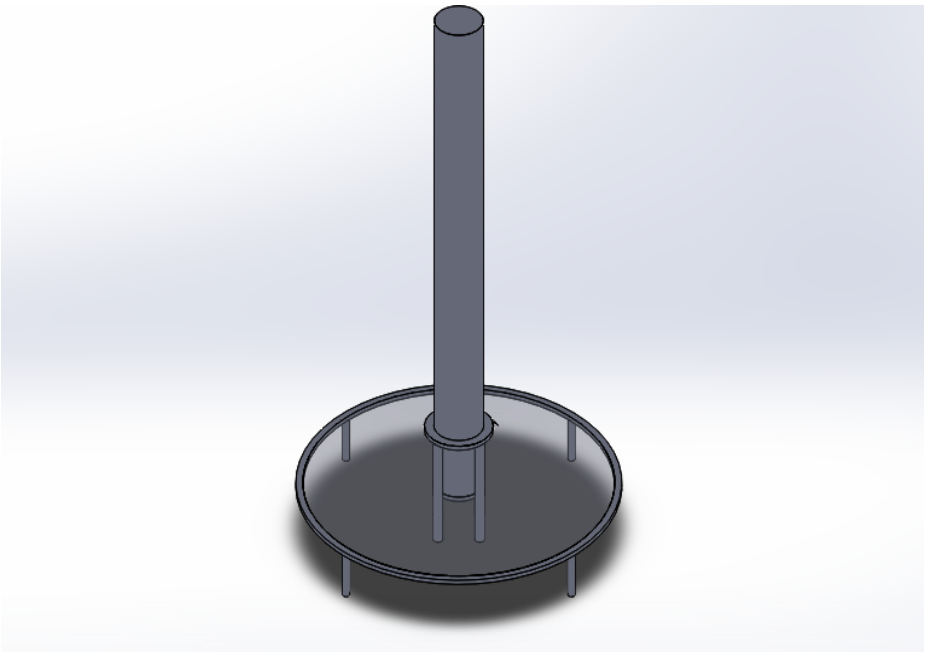

(b)

Fig. 3.3. 3D CAD model of experimental setup (a) Fron View (b) Isometric View

3.4.2. Numerical Analysis

A 2D model was modeled to save time in computations & thus making analysis simpler. 2D model was developed based on the dimensions chosen for experimental setup. A chimney height of 0.95 m, chimney diameter of 0.207 m, collector height at entry & exit of 0.2 m & 0.5 m respectively were taken into consideration as the dimensions of solar power chimney. ANSYS Design Modeler was utilized to form the physical boundary of the model.

The flow of air is due to the natural convection and is induced due to density variations. To distinguish the flow as laminar or turbulent, Rayleigh number is calculated as follows

$$\mathrm{Ra} = \frac{g\beta\Delta T L^3 \rho}{\mu\alpha} \tag{12}$$

Past studies show that flow is turbulent if Ra> 10^{10} (Gholamalizadeh & Kim, 2014) .

The following Governing Equations are implemented in numerical analysis (Amudam & Chandramohan, 2019):

Continuity Equation:

$$\nabla.(\rho\vec{v}) = 0 \tag{13}$$

Momentum Equation:

$$\nabla.(\rho\vec{v}\vec{v}) = -\nabla p + \rho\vec{g} \tag{14}$$

Energy Equation:

$$\nabla.\left(\vec{v}(\rho E + p)\right) = -\nabla.\left(\sum_j h_j J_j\right) + S_h \tag{15}$$

Since Ra > 10^{10}, therefore it is a clear-cut condition of turbulent flow and thus Realizable k-εturbulence model was used which has shown significant improvements in describing the flow (ANSYS, 2015).

Equation for turbulent kinetic energy (k):

$$\frac{\partial}{\partial X_j}(\rho k u_j) = \frac{\partial}{\partial x}\left[\left(\mu + \frac{\mu_t}{\sigma_k}\right)\frac{\partial k}{\partial X_j}\right] + G_k + G_b - \rho\varepsilon - Y_M \tag{16}$$

Equation for turbulent dissipation (ε):

$$\frac{\partial}{\partial X_j}(\rho\varepsilon u_j) = \frac{\partial}{\partial X_j}\left[\left(\mu + \frac{\mu_t}{\sigma_\varepsilon}\right)\frac{\partial \varepsilon}{\partial X_j}\right] + \rho C_1 S_\varepsilon - \rho C_2 \frac{\varepsilon^2}{k+\sqrt{\vartheta\epsilon}} + C_{1\varepsilon}\frac{\varepsilon}{k}C_{3\varepsilon}G_b \tag{18}$$

$$\mu_t = \rho C_\mu \frac{k^2}{\varepsilon} \tag{19}$$

Table 3.4

Constants used in Realizable k - ε numerical model

Model Constants	**Value**
C2-ε	1.9
TKE Pr No.	1.0
TDR Pr No.	1.2

Model Constants	**Value**
Energy Prandtl Number	0.85
Wall Prandtl Number	0.85

Mesh was generated using ANSYS FLUENT. The mesh has been refined to avoid the problem of possible Boundary Layer Separation and smoothing is kept as medium. The total number of nodes and elements are 57616 and 56827 respectively. A magnified view of mesh is represented in Fig. 3.5.

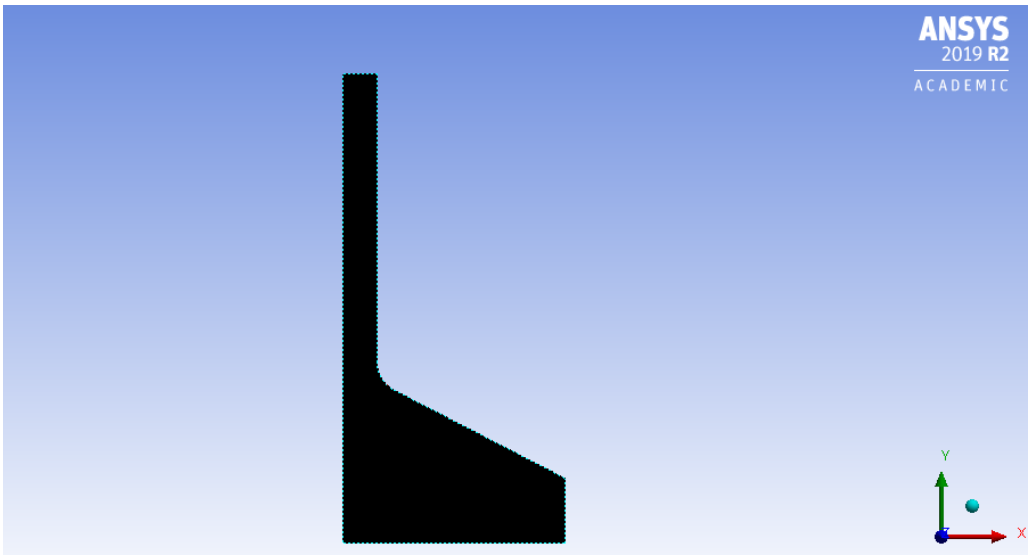

Fig. 3.4. Meshed geometry of the 2D domain

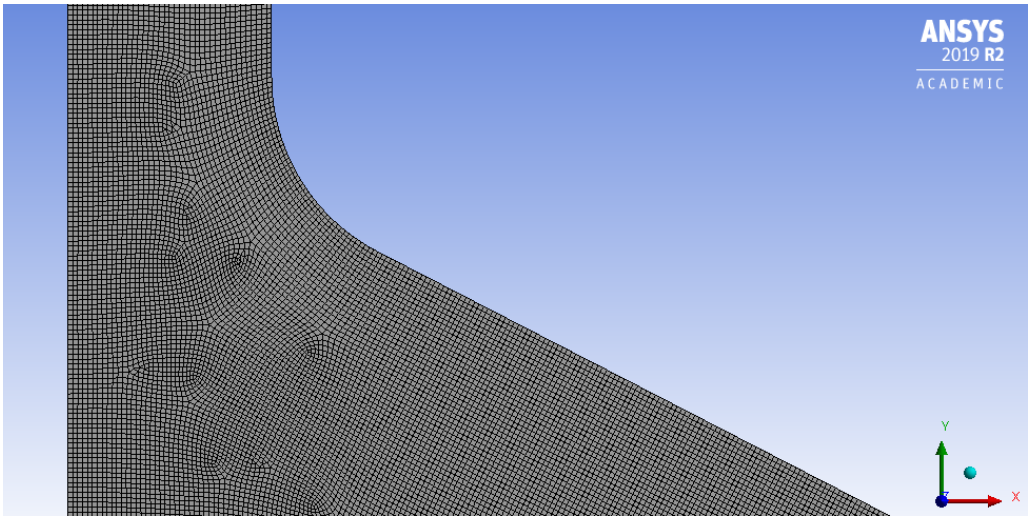

Fig. 3.5. Magnified view at collector outlet and chimney inlet

Numerical model was solved selecting steady state pressure-based solver. Since the flow is against the gravity and therefore a negative value of acceleration due to gravity is input in y-direction. Realizable k-ε turbulence model with standard wall

functions and full buoyancy effect has been setup for the analysis. The driving force in a solar chimney power plant is based on difference of density i.e. buoyancy driven air flow. Therefore, Boussinesq buoyancy model is chosen as it is applicable for small density differences (Xu & Zhou, 2018).

Table 3.5

Boundary conditions applied to the model for the analysis (Xu & Zhou, 2018)

Component	**Boundary Type**	**Boundary Conditions**
Collector	Wall type	Thermally Insulated
Collector Inlet	Pressure Inlet type	P_{gauge} = 0 bar
Collector Outlet	Pressure Outlet	P_{gauge} = 0 bar
Absorber	Wall type	Heat Flux($q^{"}$)
Tower/Chimney	Wall type	Insulated
Centerline	Axis type	-

SIMPLE algorithm was opted as the pressure-velocity coupling scheme and to maintain the accuracy of results, second order upwind was selected for pressure, momentum, turbulent kinetic energy, turbulent dissipation rate and energy(Hassan et al., 2018). The standard initialization is used as an initialization method. All variables were introduced with an initial value of zero except the temperature with an initial value of 300 K. Calculations were run for 500 repetitions for ensuring that solution is converged and all residual values reaches to a convergence state. Solution become converged at the 375^{th} iteration as shown in the Fig. 3.6.

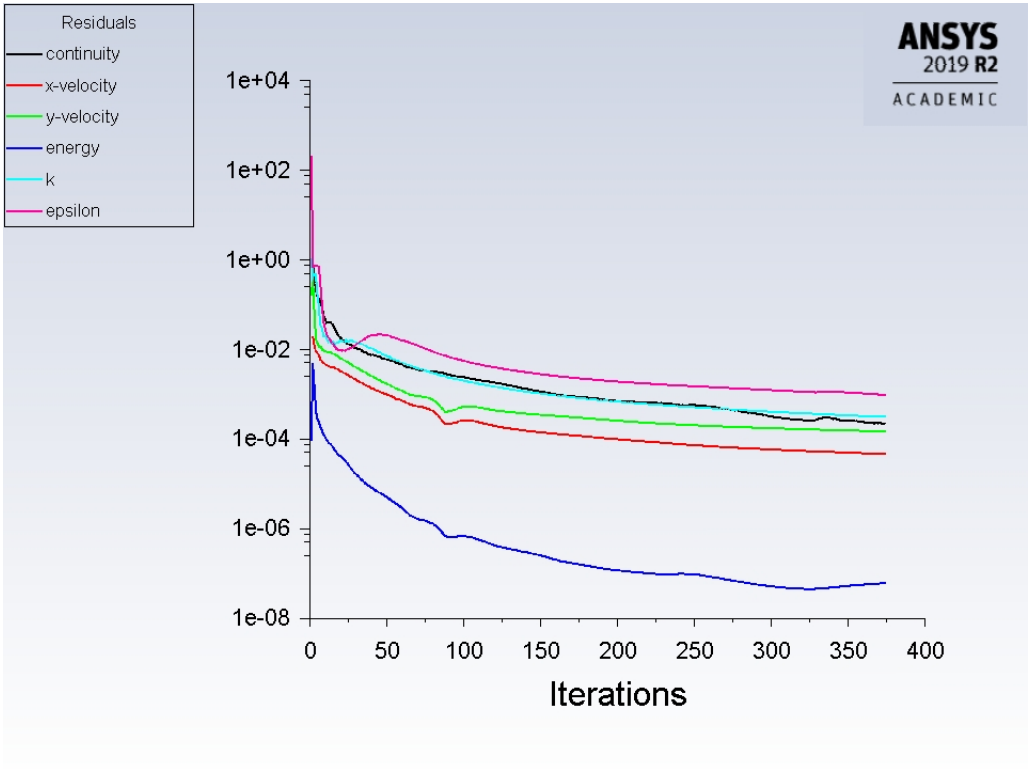

Fig. 3.6. Convergence criteria plot of the solution

CHAPTER - 4

RESULTS & DISCUSSIONS

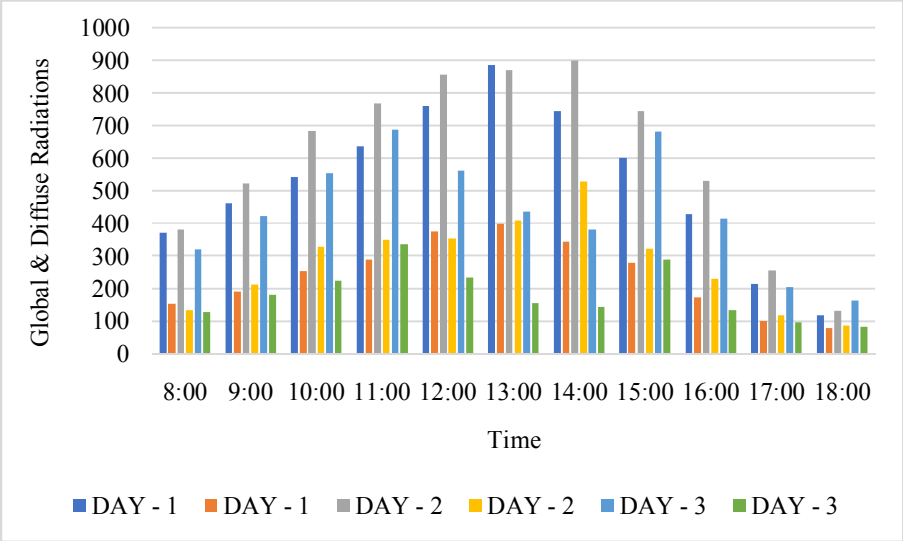

Fig. 4.1. Variation of global & diffused radiations with time

Fig. 4.1. shows the variations of global and diffused radiation for three days over a period of ten hours starting from 08:00 hrs in the morning till 18:00 hrs in the evening. It is evident from the bar graph that the maximum value of global radiation was observed on Day-2 as 901 W/m^{2}at 14:00 hrs and minimum value of global radiation was observed on all three days at 18:00 hrs. The maximum value of diffused radiation was observed as 410 W/m^2 on Day-2 at 13:00 hrs and minimum value of diffused radiation was observed on all three days at 18:00 hrs.

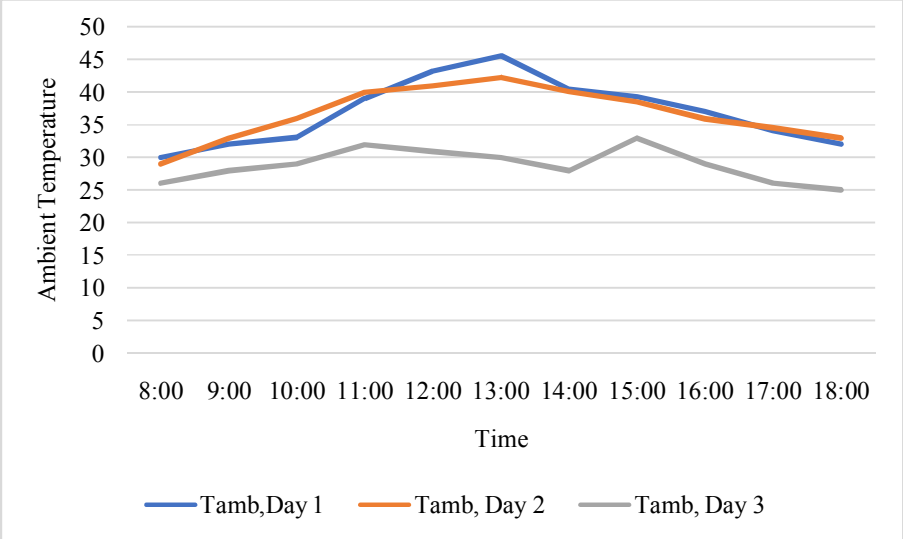

Fig. 4.2. Ambient temperature during sunshine hours

Fig. 4.2. represents ambient temperature for three days over a period of ten hours starting from 08:00 hrs in the morning till 18:00 hrs in the evening. It is evident from the graph that maximum ambient temperature of 45.6 ^{0} C was observed on Day-1 at 13:00 hrs and minimum ambient temperature of 25 ^{0} C was recorded on Day-3 at 18:00 hrs.

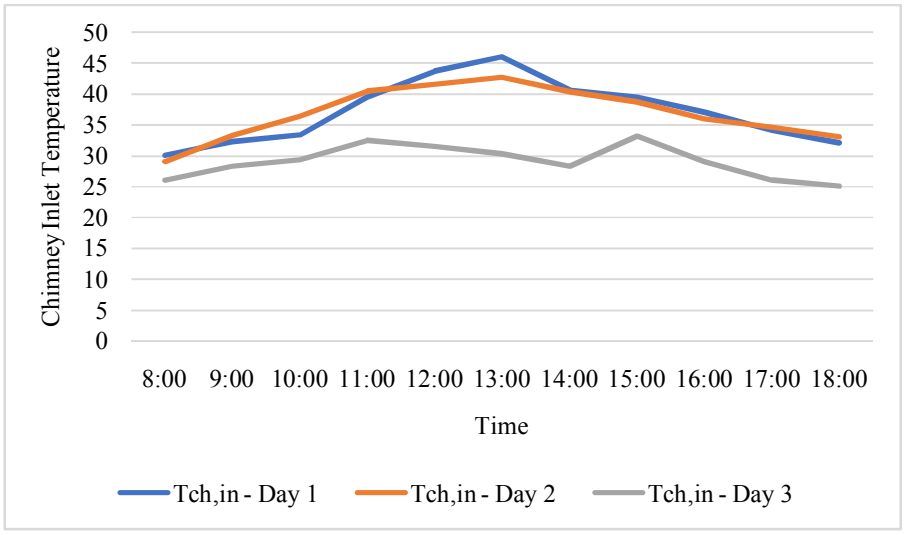

Fig. 4.3. Variation of chimney inlet air temperature

Fig. 4.3. represents chimney inlet temperature for three days over a period of ten hours starting from 08:00 hrs in the morning till 18:00 hrs in the evening. As the air flows through the collector, it picks up heat and slightly higher air temperature at the chimney inlet was observed as 46^0 C on Day-1 at 13:00 hrs. The minimum chimney inlet temperature was recorded as 25.1^0 C on Day-3 at 18:00 hrs.

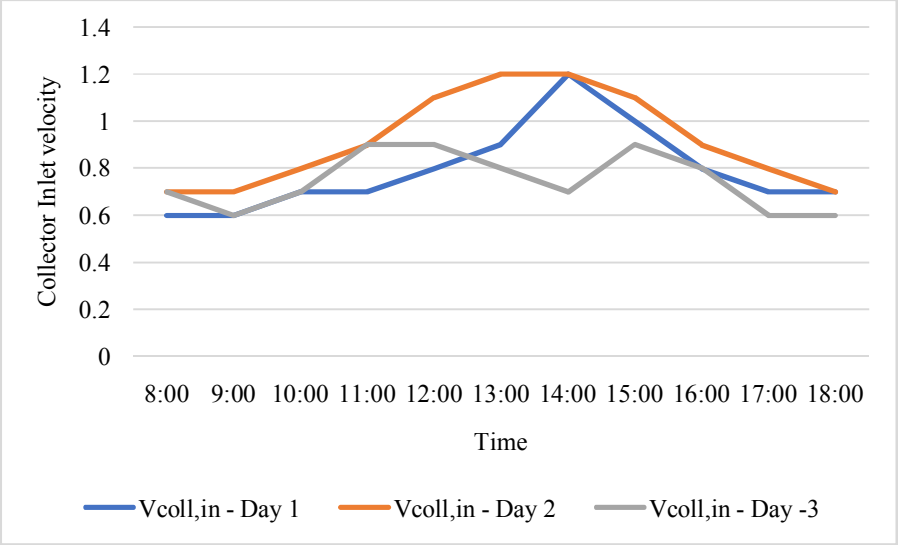

Fig. 4.4. Variation of collector inlet air velocity with time

Fig. 4.4. shows the variation of collector inlet velocity for three days over a period of ten hours starting from 08:00 hrs in the morning till 18:00 hrs in the evening. Maximum value of air velocity was observed as 1.2 m/s on Day-2 in between 13:00 hrs and 14:00 hrs while the minimum air velocity was observed as 0.6 m/s in the morning 08:00 hrs and evening 18:00 hrs. on Day-1 and Day-3 respectively.

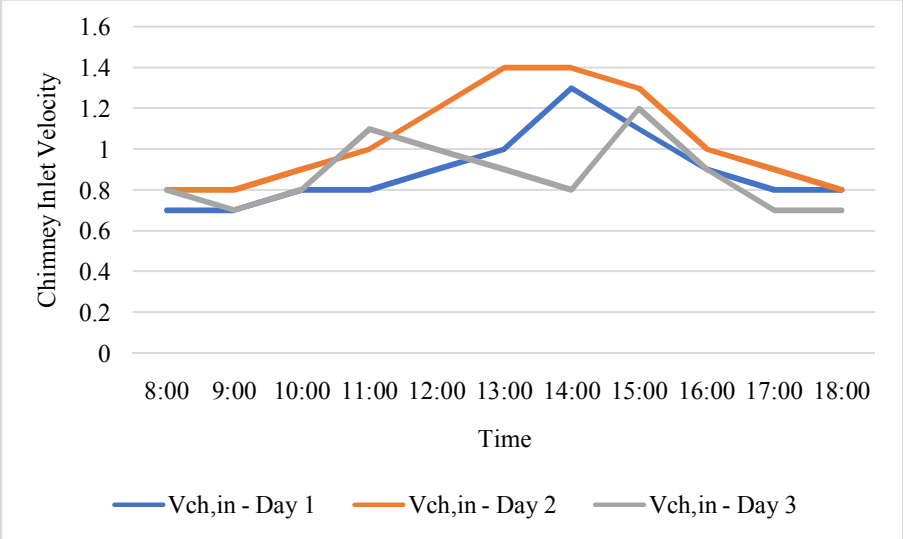

Fig. 4.5. Variation of chimney inlet air velocity with time

Fig. 4.5. Shows the variation of chimney inlet velocity for three days over a period of ten hours starting from 08:00 hrs in the morning till 18:00 hrs in the evening. Maximum value of air velocity was recorded observed as 1.4 m/s on Day-2 in between 13:00 hrs and 14:00 hrs. The minimum air velocity was recorded as 0.7 m/s.

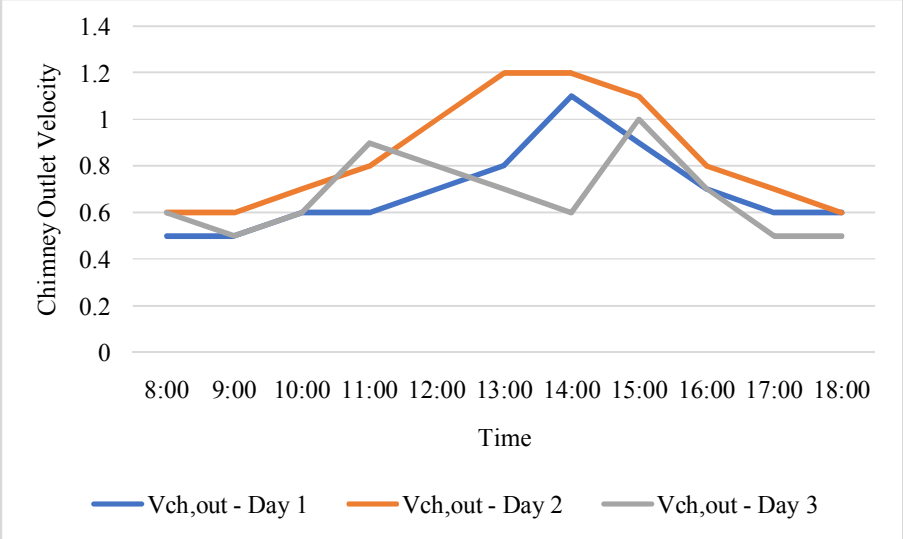

Fig. 4.6. Variation of chimney outlet air velocity with time

Fig. 4.6. Shows the variation of chimney outlet velocity for three days over a period of ten hours starting from 08:00 hrs in the morning till 18:00 hrs in the evening. As the air flows through the chimney, slight reduction in air velocity is observed. Maximum value of air velocity was observed as 1.2 m/s on Day-2 in between 13:00 hrs and 14:00 hrs and the minimum air velocity was recorded as 0.5 m/s on Day-1 & Day-2 in the morning and evening respectively.

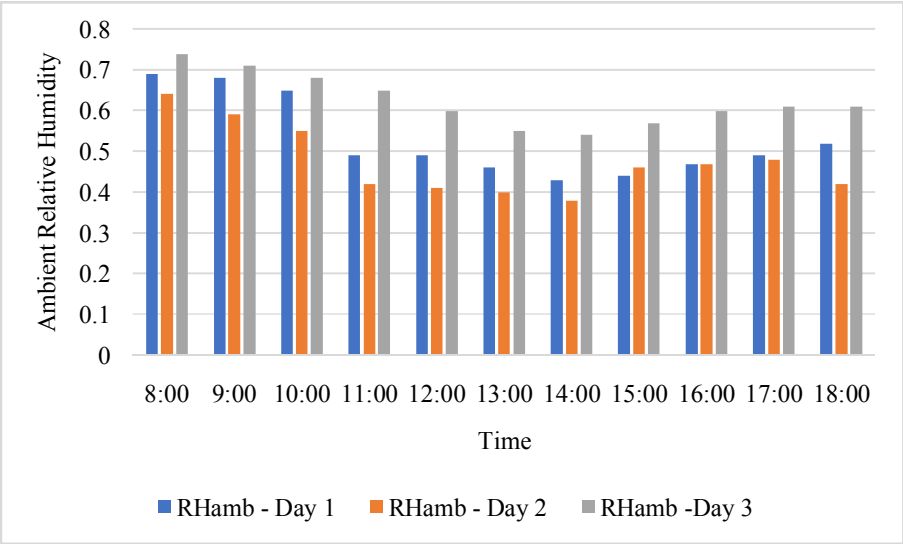

Fig. 4.7. Variation of ambient RH

Fig. 4.7. represents variation of ambient RH for three days over a period of ten hours starting from 08:00 hrs in the morning till 18:00 hrs in the evening. The maximum value of ambient RH was observed as 0.74 on Day-3 at 08:00 hrs while the minimum value of ambient RH was observed as 0.38 on Day-2 at 14:00 hrs.

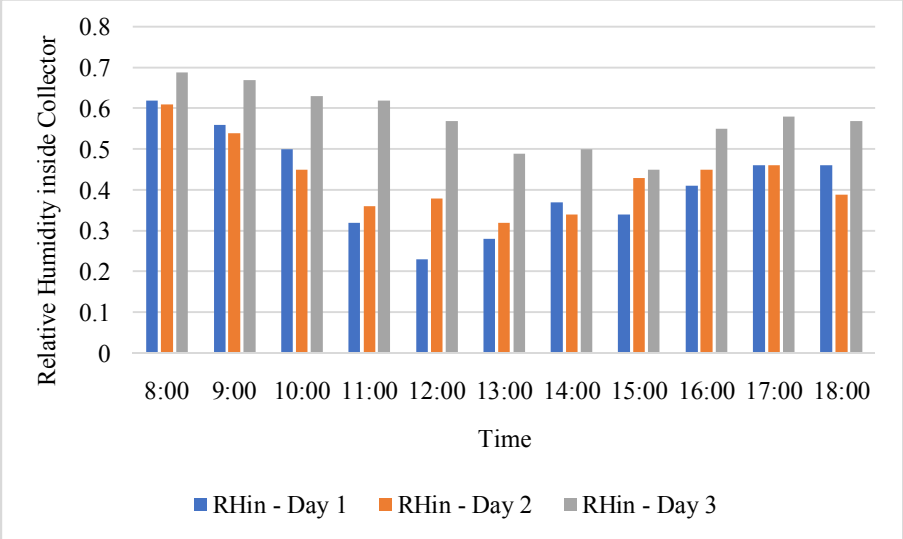

Fig. 4.8. Variation of relative humidity under the collector

Fig. 4.8. represents variation of RH under the collector for three days over a period of ten hours starting from 08:00 hrs in the morning till 18:00 hrs in the evening. The maximum value of RH was observed as 0.69 on Day-3 at 08:00 hrs while the minimum value of ambient RH was observed as 0.23 on Day-1 at 12:00 hrs.

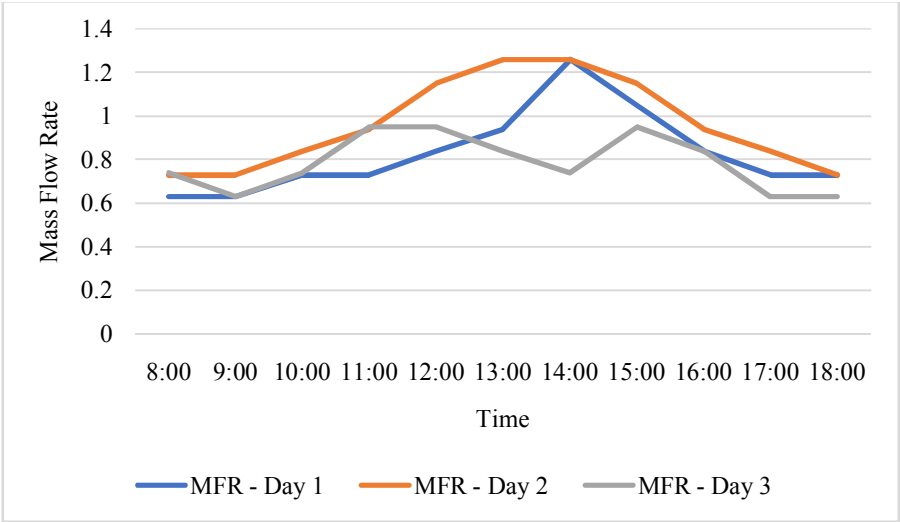

Fig. 4.9. Variation of inlet mass flow rate with time

Fig. 4.9. Shows the variation of mass flow rate at the entry to the collector for three days over a period of ten hours starting from 08:00 hrs in the morning till 18:00 hrs in the evening. The maximum value of MFR was observed as 1.26 kg/sec on Day-2 in between 13:00 hrs and 14:00 hrs. Also, the minimum value of MFR was observed as 0.63 kg/s on Day-1 & Day-2 in between 08:00 hrs&09:00 hrs.

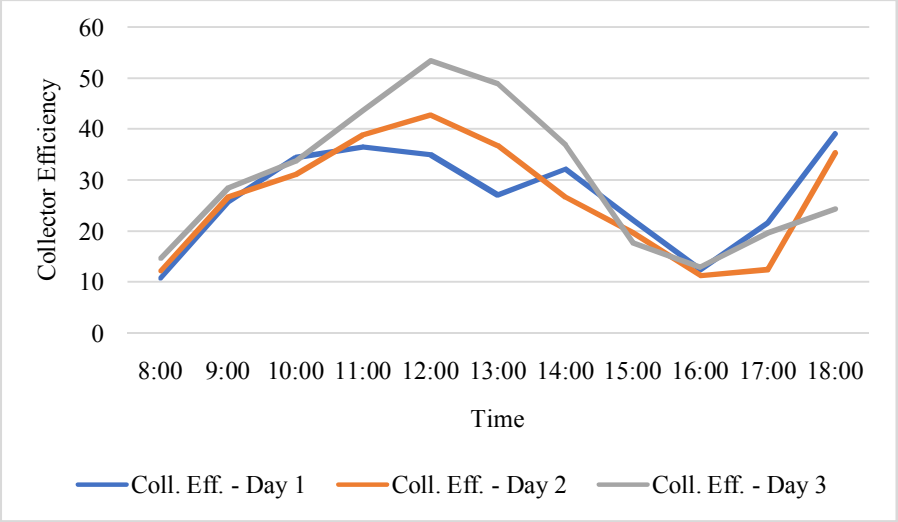

Fig. 4.10. Variation of collector efficiency with time

Fig 4.10. Shows the variation of collector efficiency for three days over a period of ten hours starting from 08:00 hrs in the morning till 18:00 hrs in the evening. A maximum collector efficiency of 53.48% on Day-3 was observed at 12:00 hrs while the minimum collector efficiency was observed as 10.74% on Day-1 at 8:00 hrs.

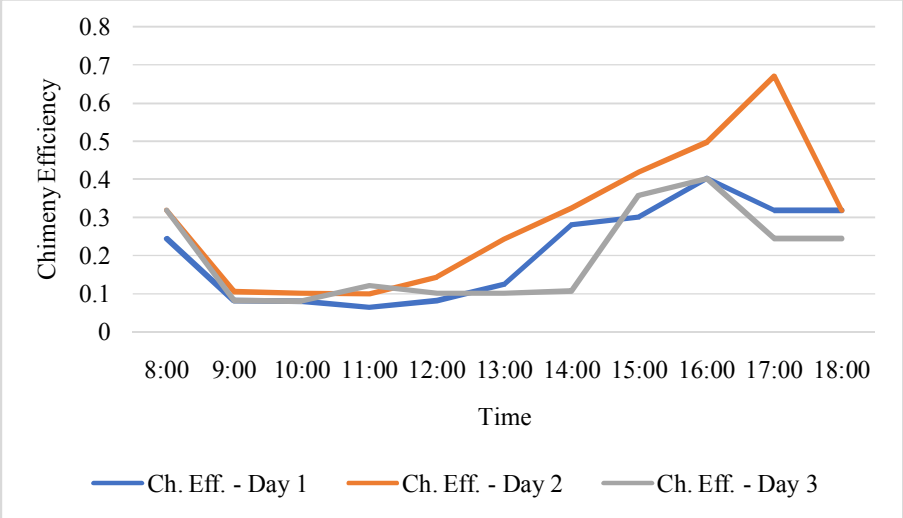

Fig. 4.11. Variation of chimney efficiency with time

Fig 4.11. Shows the variation of chimney efficiency for three days over a period of ten hours starting from 08:00 hrs in the morning till 18:00 hrs in the evening. A maximum chimney efficiency of 0.67% on Day-2 was observed at 17:00 hrs while the minimum chimney efficiency was observed as 0.06% on Day-1 at 11:00 hrs.

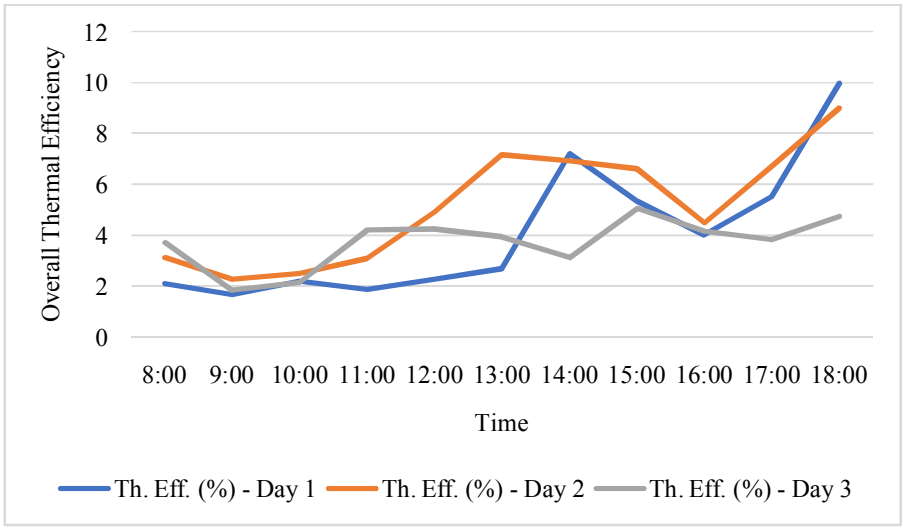

Fig. 4.12. Variation of overall thermal efficiency with time

Fig 4.12. Shows the variation of overall thermal efficiency for three days over a period of ten hours starting from 08:00 hrs in the morning till 18:00 hrs in the evening. A maximum overall efficiency of 9.98% was observed on Day-1 at 18:00

hrs while the minimum overall efficiency was observed as 1.68 % on Day-1 at 09:00 hrs.

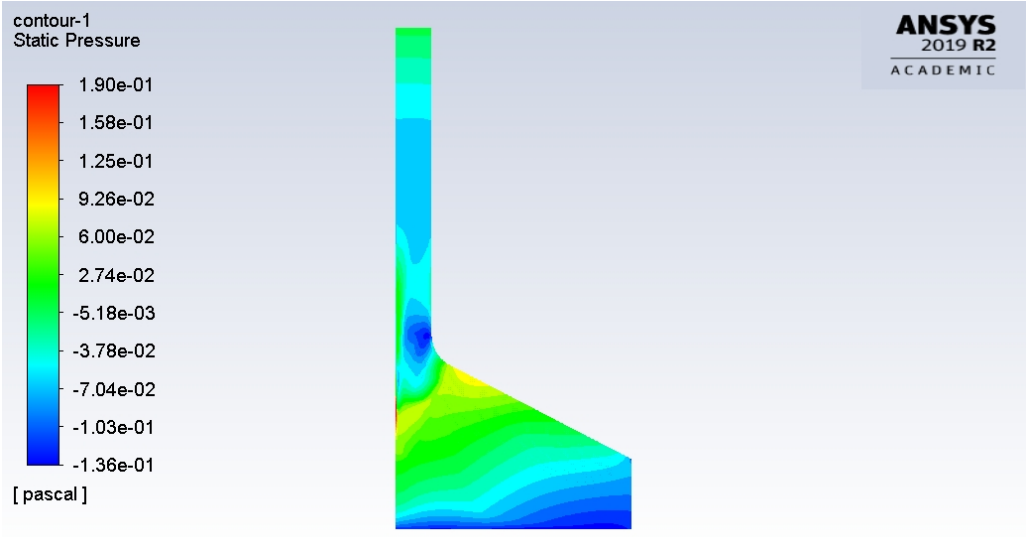

Fig. 4.13. Static Pressure contours

Fig. 4.13. Shows the variation of Static Pressure inside the solar power chimney

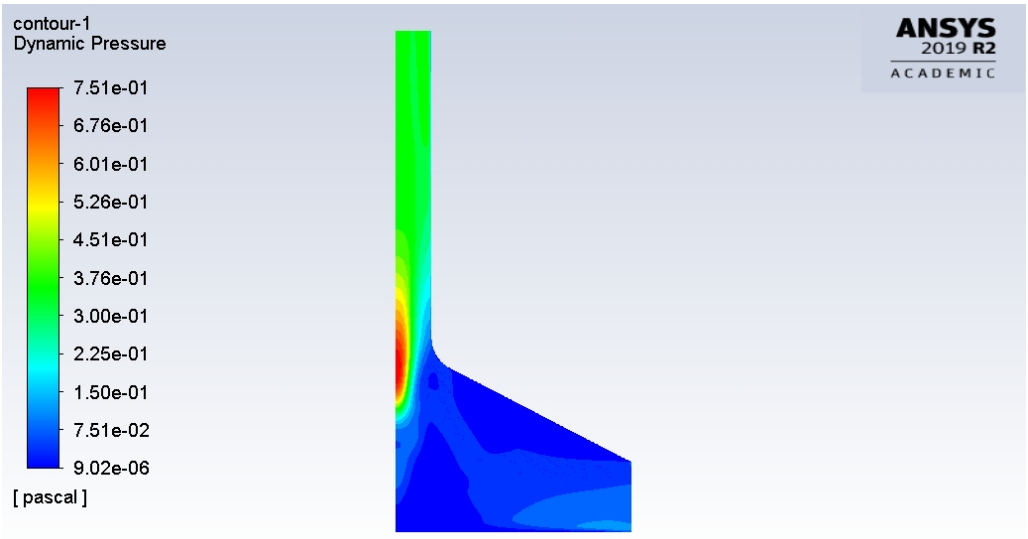

Fig. 4.14. Dynamic Pressure contours

Fig. 4.14. Shows the variation of Dynamic Pressure inside the solar power chimney

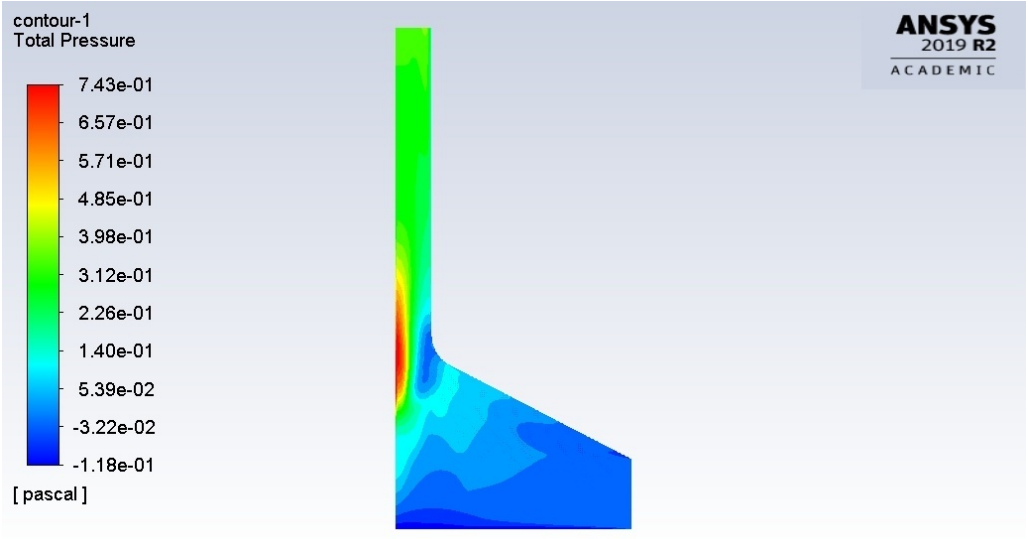

Fig. 4.15. Total Pressure contours

Fig. 4.15. Shows the variation of Total Pressure inside the solar power chimney

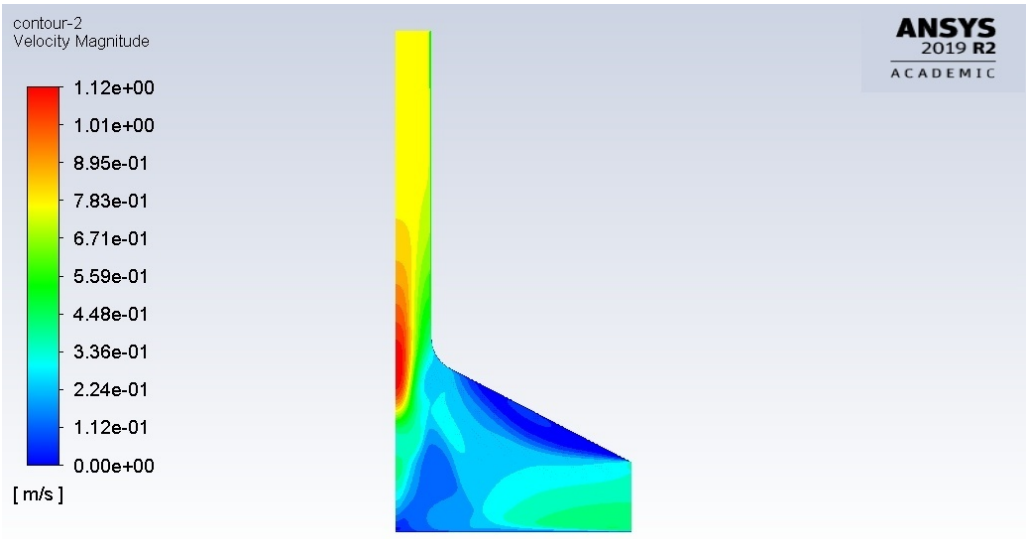

Fig. 4.16. Velocity magnitude contours

Fig. 4.16. shows that the velocity at chimney outlet is about 0.7 m/s while the velocity at collector inlet is about 0.4 m/s and therefore, trends of velocity are in line with the experimental data recorded during the experimental analysis of the solar power chimney. The velocity near the turbine inlet area as per the velocity magnitude contours is about 1.2 m/s.

CHAPTER - 5

CONCLUSIONS & RECOMMNEDATIONS

The following conclusions are drawn from the experimental and numerical analysis performed on the solar chimney power plant.

- A maximum collector efficiency of 53.48% on Day-3 was observed at 12:00 hrs while the minimum collector efficiency was observed as 10.74% on Day-1 at 8:00 hrs.
- A maximum chimney efficiency of 0.67% on Day-2 was observed at 17:00 hrs while the minimum chimney efficiency was observed as 0.06% on Day-1 at 11:00 hrs.
- A maximum overall efficiency of 9.98% was observed on Day-1 at 18:00 hrs while the minimum overall efficiency was observed as 1.68 % on Day-1 at 09:00 hrs.
- The maximum value of MFR was observed as 1.26 kg/sec on Day-2 in between 13:00 hrs and 14:00 hrs. Also, the minimum value of MFR was observed as 0.63 kg/s on Day-1 & Day-2 in between 08:00 hrs&09:00 hrs.
- Trends of velocity in the numerical analysis are in line with the experimental data recorded during the experimental analysis of the solar power chimney. The velocity near the turbine inlet area as per the velocity magnitude contours is about 1.2 m/s.

REFERNCES

1. Amudam, Y., & Chandramohan, V. P. (2019). Influence of thermal energy storage system on flow and performance parameters of solar updraft tower power plant: A three dimensional numerical analysis. Journal of Cleaner Production, 207, 136–152. https://doi.org/10.1016/j.jclepro.2018.09.248
2. ANSYS. (2015). ANSYS Fluent Theory Guide. Release 16.0. ANSYS Inc . Canonsburg, Pennsylvania.
3. A. W. Culp. *Principles of Energy Conversion*. 2nd ed. McGraw-Hill, New York, 1991.
4. Breeze, P. (2005). 13: Solar power. In Power Generation Technologies (pp. 184–203). https://doi.org/10.1016/B978-075066313-7/50014-0
5. Çengel & Boles (2015). *Thermodynamics: An Engineering Approach.* McGraw-Hill.
6. Chauhan, P. S., & Kumar, A. (2017). Heat transfer analysis of north wall insulated greenhouse dryer under natural convection mode. Energy, 118, 1264–1274. https://doi.org/10.1016/j.energy.2016.11.006
7. Eryener, D., & Kuscu, H. (2018). Hybrid transpired solar collector updraft tower. Solar Energy, 159(November 2017), 561–571. https://doi.org/10.1016/j.solener.2017.11.035
8. Fadaei, N., Kasaeian, A., Akbarzadeh, A., & Hashemabadi, S. H. (2018). Experimental investigation of solar chimney with phase change material (PCM). Renewable Energy, 123, 26–35. https://doi.org/10.1016/j.renene.2018.01.122
9. Fathi, N., McDaniel, P., Aleyasin, S. S., Robinson, M., Vorobieff, P., Rodriguez, S., & Oliveira, C. de. (2018). Efficiency enhancement of solar chimney power plant by use of waste heat from nuclear power plant. Journal of Cleaner Production, 180, 407–416. https://doi.org/10.1016/j.jclepro.2018.01.132
10. Gannon, A. J., & Backström, T. W. (2003). Solar Chimney Turbine Performance. J. Sol. Energy Eng 125(1) , 101-106.
11. Gholamalizadeh, E., & Kim, M.-H. (2014). Three-dimensional CFD analysis for simulating the greenhouse effect in solar chimney power plants using a two-band radiation model. Renewable Energy , Vol. 63, 498-206.

12. Haaf, W., Friedrich, K., Mayr, G., & Schlaich, J. (1983). Solar chimneys, part I: principle and construction of the pilot plant in Manzanares. Int. J. Solar Energy 2, , 3-20.
13. Hassan, A., Ali, M., & Waqas, A. (2018). Numerical investigation on performance of solar chimney power plant by varying collector slope and chimney diverging angle. Energy, 142, 411–425. https://doi.org/10.1016/j.energy.2017.10.047
14. Jafarifar, N., Behzadi, M. M., & Yaghini, M. (2019). The effect of strong ambient winds on the efficiency of solar updraft power towers: A numerical case study for Orkney. Renewable Energy, 937–944. https://doi.org/10.1016/j.renene.2019.01.058
15. Jebasingh, V. K., & Herbert, G. M. J. (2016). A review of solar parabolic trough collector. Renewable and Sustainable Energy Reviews, 54, 1085–1091. https://doi.org/10.1016/j.rser.2015.10.043
16. Kalash, S., Naimeh, W., & Ajib, S. (2013). Experimental investigation of the solar collector temperature field of a sloped solar updraft power plant prototype. Solar Energy, 98, 70–77. https://doi.org/10.1016/j.solener.2013.05.025
17. Kalash, S., Naimeh, W., & Ajib, S. (2014). Experimental investigation of a pilot sloped solar updraft power plant prototype performance throughout a year. Energy Procedia, 50, 627–633. https://doi.org/10.1016/j.egypro.2014.06.077
18. Kalogirou, S. A. (2004). Solar thermal collectors and applications (Vol. 30). https://doi.org/10.1016/j.pecs.2004.02.001
19. MNRE. (2018). ANNUAL REPORT 2017-18. New Delhi: Ministry of New and Renewable Energy.
20. Najm, O. A., & Shaaban, S. (2018). Numerical investigation and optimization of the solar chimney collector performance and power density. Energy Conversion and Management, 168(January), 150–161. https://doi.org/10.1016/j.enconman.2018.04.089
21. Nizetic, S., & Klarin, B. (2010). A simplified analytical approach for evaluation of the optimal ratio of pressure drop across the turbine in solar chimney power plants. Applied Energy, 87(2), 587–591. https://doi.org/10.1016/j.apenergy.2009.05.019
22. Schlaich, J., & Schiel, W. (2003). Solar Chimneys. In Encyclopedia of Physical Science and Technology (Third Edition) (pp. 99–109).

https://doi.org/10.1201/9781420039924.ch4

23. Schlaich, J. (1995). The Solar Chimney: Electricity From the Sun. Stuttgart , Germany: Edition Axel Menges.
24. Schlaich, J., & Bergermann, R. (2018, December 1). Prototype-Manzanares. Retrieved December 1, 2018, from www.solar-updraft-tower.com: https://www.solar-updraft-tower.com/concept/prototype-manzanares/
25. Wikipedia Contirbutors. (2018, November 4). Solar updraft tower. (Wikipedia, The Free Encyclopedia.) Retrieved December 1, 2016, from https://en.wikipedia.org/w/index.php?title=Solar_updraft_tower&oldid=867308887
26. Winston, R. (1974). Principle of Solar Concentrators of a Novel Design. Solar Energy, 16(1), 89–95.
27. Xu, Y., & Zhou, X. (2018). Performance of divergent-chimney solar power plants. Solar Energy, 170(October 2017), 379–387. https://doi.org/10.1016/j.solener.2018.05.068
28. Zhou, X., Wang, F., Fan, J., & Ochieng, R. M. (2010). Performance of solar chimney power plant in Qinghai-Tibet Plateau. Renewable and Sustainable Energy Reviews, 14(8), 2249–2255. https://doi.org/10.1016/j.rser.2010.04.017
29. Zhou, X., & Xu, Y. (2016). Solar updraft tower power generation. Solar Energy, 128, 95–125. https://doi.org/10.1016/j.solener.2014.06.029
30. Zhou, X., Yang, J., Wang, J., & Xiao, B. (2009). Novel concept for producing energy integrating a solar collector with a man made mountain hollow. Energy Conversion and Management, 50(3), 847–854. https://doi.org/10.1016/j.enconman.2008.09.006
31. Zhou, X., Yang, J., Xiao, B., & Hou, G. (2007). Experimental study of temperature field in a solar chimney power setup. Applied Thermal Engineering, 27(11–12), 2044–2050. https://doi.org/10.1016/j.applthermaleng.2006.12.007
32. Zhou, X., Yuan, S., & Bernardes, M. A. D. S. (2013). Sloped-collector solar updraft tower power plant performance. International Journal of Heat and Mass Transfer, 66, 798–807. https://doi.org/10.1016/j.ijheatmasstransfer.2013.07.060

APPENDIX - A

INDIAN ENERGY SCENARIO

The total current installed capacity of India as on date 31.05.2019 given by Central Electricity Authority is 356.818 GW. It is evident from the table given below that India is still heavily dependent upon conventional sources of energy with a share of more than sixty percent in which coal has a maximum share of about 54.5 percent followed by the Gas and Oil. The renewable sources of energy contribute close to about 35 percent whereas nuclear energy is at the bottom with a share of only 1.9 percent.

Table A.1
Total Installed capacity in India

Source – RES (MNRE) as on 30.04.2019

S.No.	Fuel	MW	Percentage of Total
1.	Thermal Energy	2,26,279	63.4%
	• Coal	1,94,445	54.5%
	• Gas	24,937	7.0%
	• Oil	638	0.2%
2.	Hydro Energy (Renewable)	45,399	12.7%
3.	Nuclear Energy	6,780	1.9%
4.	Other	78,359	22.0%
Total		**3,56,818**	**100%**

Table A.1 represents the total installed capacity of India with major share of thermal energy being 63.4%.

The contribution of the various sectors in total installed capacity is given in the Table A.2. given below. The maximum contribution is by the Private sector followed by the Central and State sector.

Table A.2

Share of Various sector in Total Installed Capacity (As on 31.05.2019)

Source – Central Electricity Authority (CEA)

S.No.	Sector	MW	% of Total
1.	State	86,597	24.3%
2.	Central	105,077	29.4%
3.	Private	165,144	46.3%
Total		**3,56,818**	**100%**

Over the years India is taking certain steps to promote renewable energy and investing in it for the sustainable use of resources for future generations. Along with the grid power, a decentralized distributed electrification system using renewable systems can provide low budget options for cooking, lighting, and energy uses in rural areas. Renewable energy plays important role in reducing carbon emissions and consumption of fossil fuels. With the help of international support, India has a target to increase fossil free based installed power capacity to 40 percent with the end of the year 2030. India is also focusing on to reduce Green House Gas emissions and further increasing the green cover for absorbing CO_2. With an aim to become a global leader in the solar energy sector, the National Solar Mission was launched in January 2010. Rooftop solar system and solar water heaters are being promoted by providing subsidies from the central government.

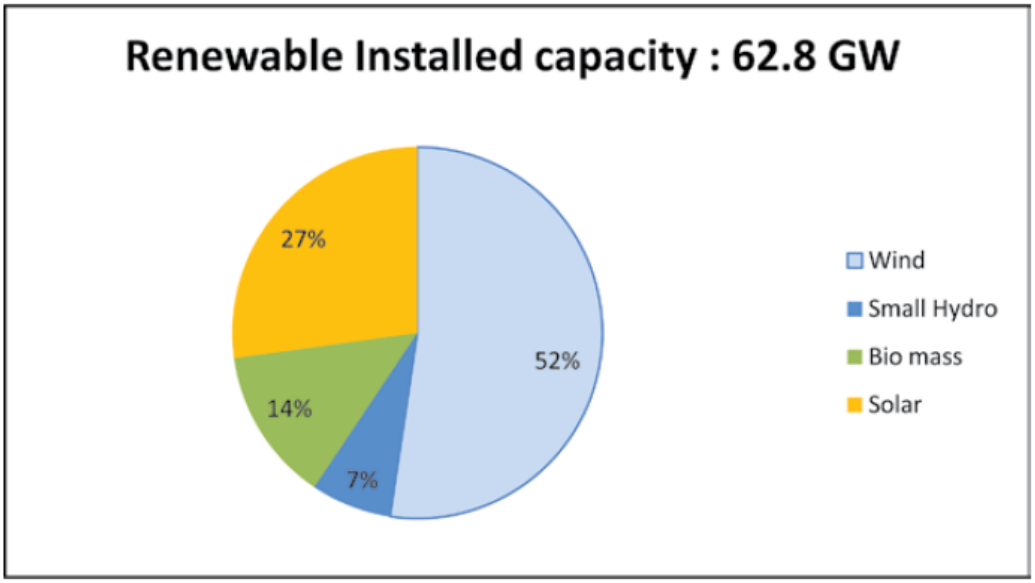

Fig. A.1. Renewable energy installed capacity (MNRE, 2018)

Renewable energy is capable enough to mark new beginning for the universal energy needs. India which is close to the equator has great potential to harness energies like wind energy, small hydropower plant, tidal energy wave, energy and Ocean Thermal Energy Conversion (OTEC). Renewable energy can provide viable solutions for the unelectrified village areas which are still energy-deprived. India has been overall ranked fourth-largest power producer in the world.

ISA (International Solar Alliance)

It is an international intergovernmental organization headquartered in India. ISA secretariat is located on the campus of the National Institute of Solar Energy, Gwalpahari, Gurugram, Haryana, India. Under the Indian leadership, it was launched together by French president and PM, India on Nov 30, 2018, in Paris, France which is in agreement with COP-21. The main motive is to address the issues for deployment of solar energy through coordination among the solar efficient countries which lies near about equator.

APPENDIX - B

MINISTRY OF NEW & RENEWABLE ENERGY (MNRE)

Institutions under the MNRE

There are total five institutions that forms the backbone of the Ministry and includes two Public Sector Undertakings (PSU) and three autonomous bodies.

1. **Indian Renewable Energy Development Agency** – It is a Non-Banking Financial Institution based in New Delhi and provided loans for renewable energy.
2. **Solar Energy Corporation of India** – It is a Section 3 company under the Companies Act, based in New Delhi and assists in administration of NSM.
3. **National Institute of Solar Energy** – It is located at Gwal Pahari district, Gurugram, Haryana and this apex institute is involved in R&D activties.
4. **National Institute of Wind Energy** – It is situated in Chennai, India & is the only dedicated institute for R&D of wind power
5. **National Institute of Bio-Energy** – It is located in the district of Kapurthala, Punjab and focused on research & development in Biofuel based energy.

Apart from these five institutions Alternate Hydro Energy Centre (AHEC) and IIT Roorkee also provide assistance for the development of small hydropower projects.

Table B.1

Institutions under the MNRE

S.No.	Institution	Abbreviation	Type of Institution	Location
1.	Solar Energy Corporation of India	SECI	PSU	NCT
2.	National Institute of Wind Energy	NIWE	Autonomous	Chennai, Tamil Nadu
3.	Indian Renewable Energy Development Agency	IREDA	PSU	NCT
4.	National Institute of BioEnergy	NIBE	Autonomous	Kapurthala, Punjab
5.	National Institute of Solar Energy	NISE	Autonomous	Gurugram, Haryana

APPENDIX - C

SOME FACTS & FIGRUES ABOUT INDIAN ENERGY SECTOR

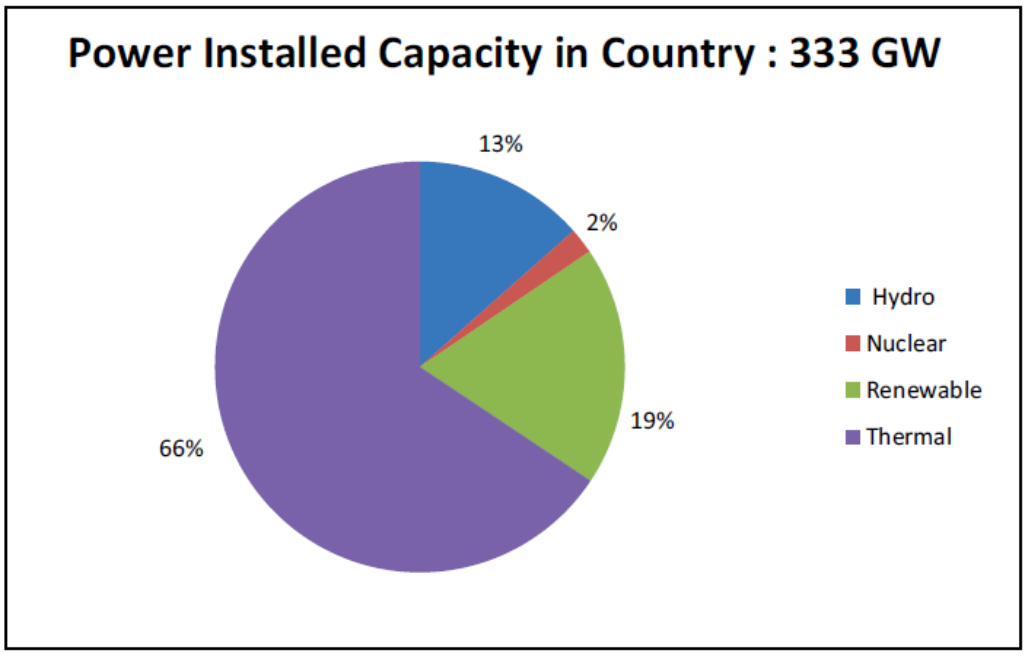

Fig. C.1. Total Installed Capacity in India (MNRE, 2018)

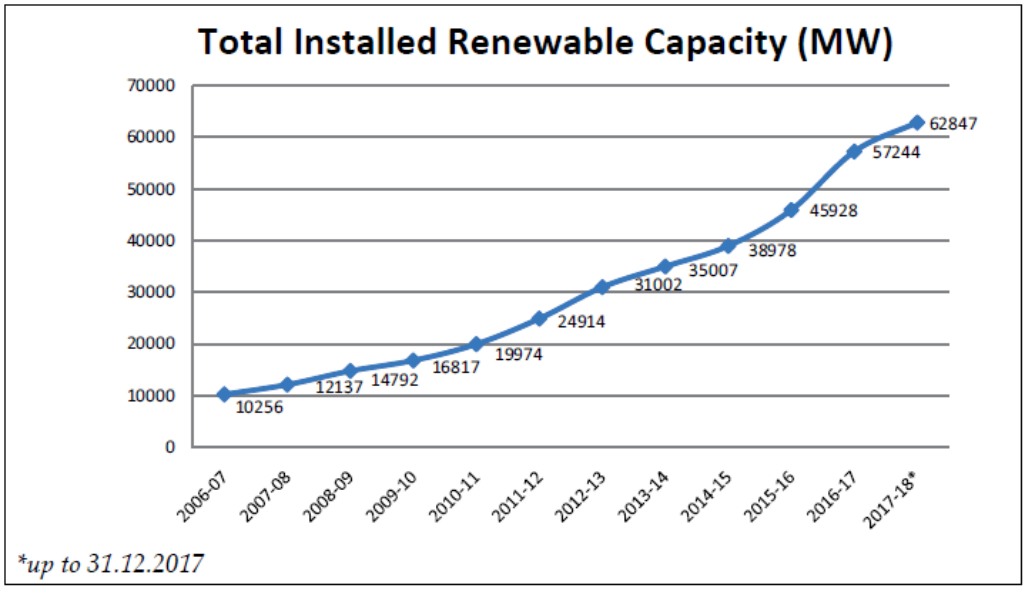

Fig. C.2. Total Installed Renewable Capacity in India for a period of 12 years (MNRE, 2018)

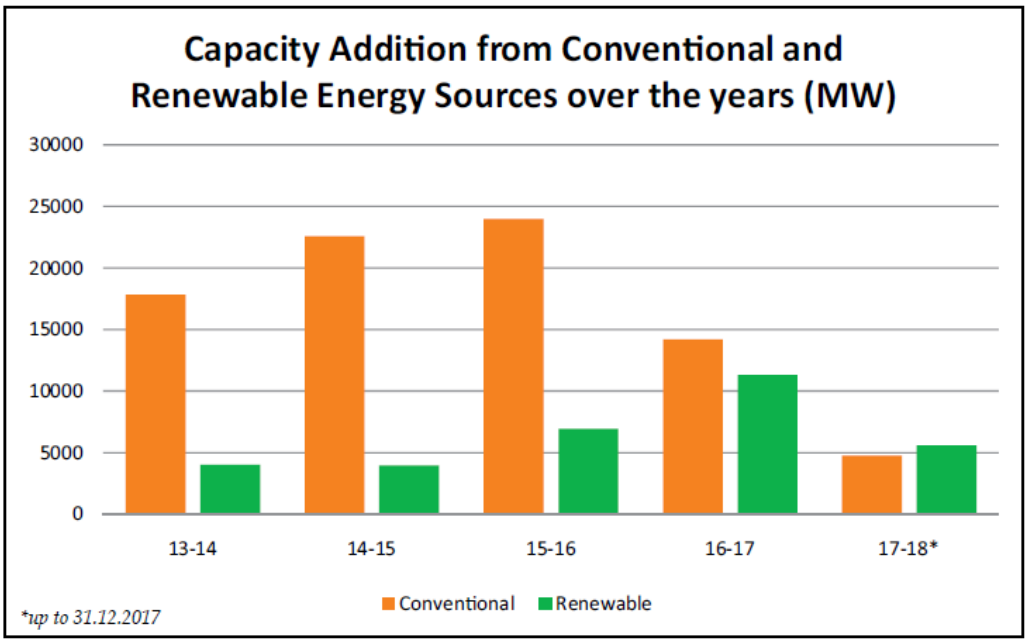

Fig. C.3. Capacity addition renewable and conventional sources of energy (MNRE, 2018)

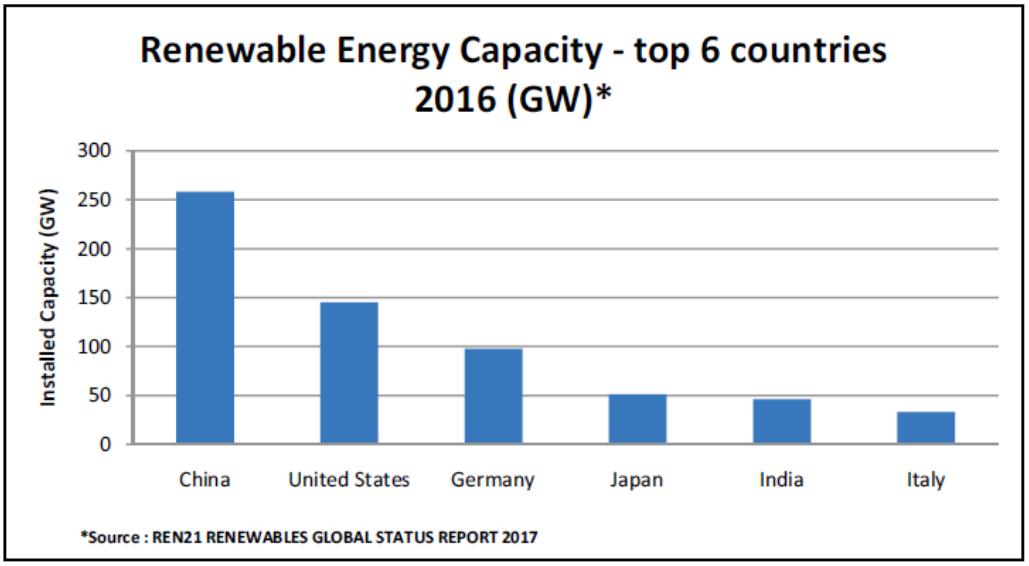

Fig. C.4. Top 6 countries in Renewable Energy capacity (MNRE, 2018)

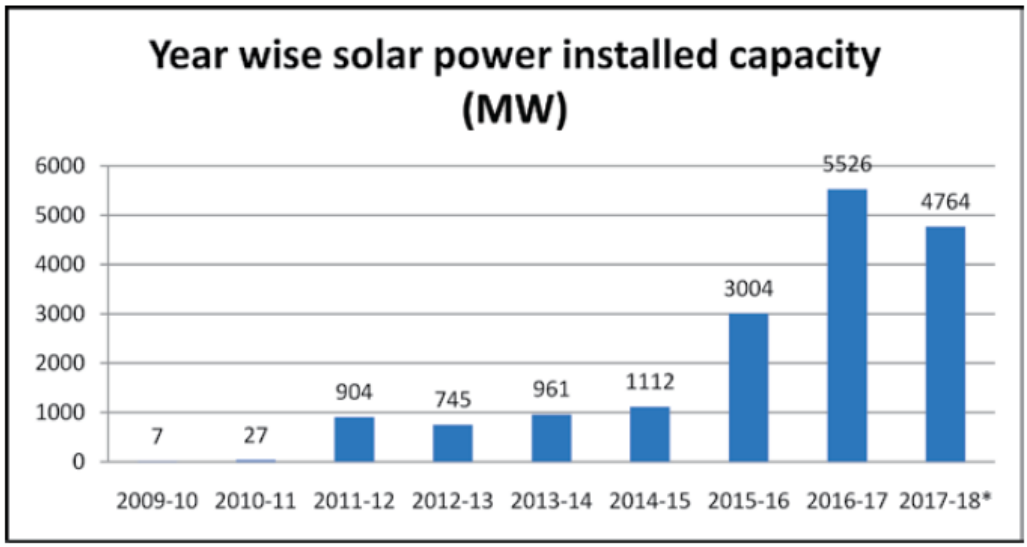

Fig. C.5. Year wise solar power installed capacity (MNRE, 2018)

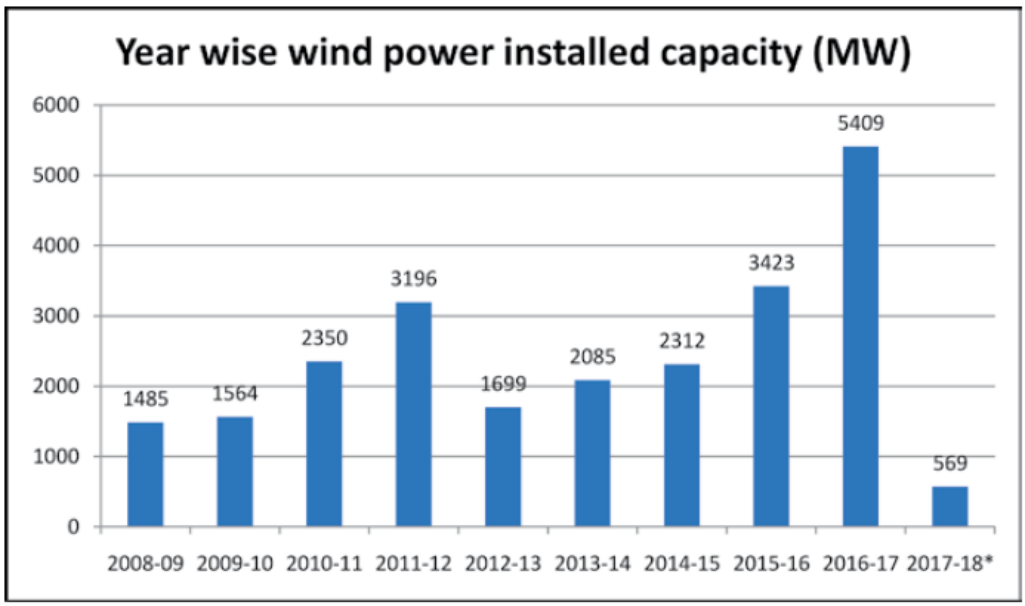

Fig. C.6. Year wise wind power installed capacity (MNRE, 2018)

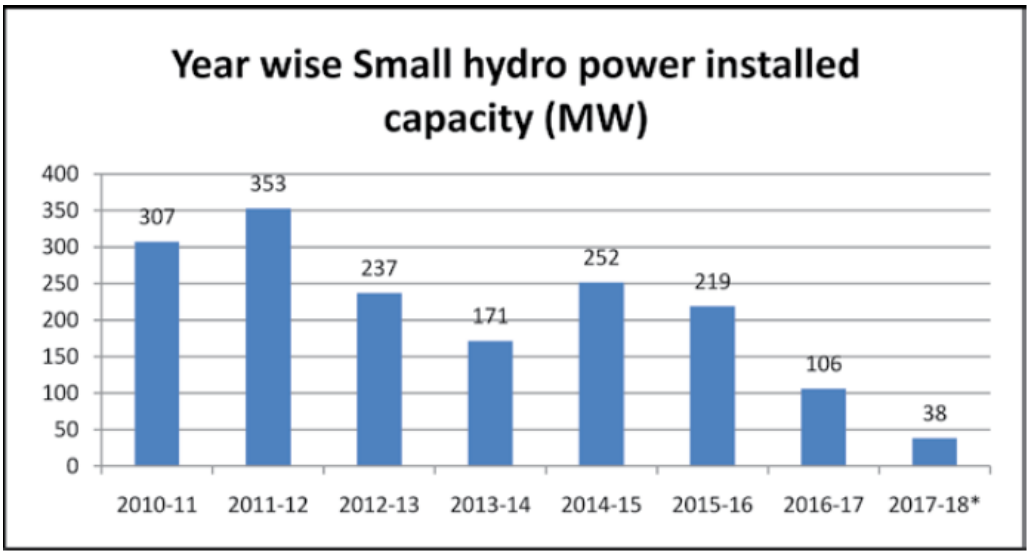

Fig. C.7. Year wise Small hydro power installed capacity (MNRE, 2018)